공학박사학위논문

전기자동차용 열펌프시스템의 한냉시 운전성능 향상

Performance improvement of heat pump system during cold climate operation for electric vehicle application

2017년 8월

서울대학교 대학원

기계항공공학부

권 춘 규

Abstract

Performance improvement of heat pump system during cold climate operation for electric vehicle application

Chunkyu Kwon

Department of Mechanical and Aerospace Engineering

The Graduate School

Seoul National University

Battery-powered electric vehicles(EVs) need an efficient electric heating system for extending the driving mileage. An air-source heat pump system offers an economical alternative for electric vehicles because it consumes less energy than a heating system using Joule heat and it can use the same components as an air conditioning system for cooling. However, its performance degradation is inevitable at very low ambient temperature (cold climate condition). Although EV applies the heat pump system, it needs additional electric heater like high voltage positive temperature coefficient (PTC) heater. It does raise cost a lot, but also makes the vehicle package more complex. Therefore the heating performance improvement of heat pump during cold climate is very important theme. This has been studied a lot in the residential or industrial heat pump, but the cold climate heat pump (CCHP) for EV application is quite limited. In this study, we tried to investigate the cold climate heat pmp for electric vehicle application. The configuration of a vapor injection heat pump, which was well known as a good technology to

overcome this problem in residential heat pump systems, was introduced and the performance characteristics were studied using a scroll compressor geometry-based thermodynamic analysis. And three types of cold climate heat pump (CCHP) were proposed to improve the heat pump performance in cold climate, and were experimentally evaluated for electric vehicle application. These experiments were system-level tests. To validate the real electric vehicle heating performance considering transient performance, in other words, the cabin thermal load change during soak and warm-up process, we installed the cold climate heat pump (CCHP), which was chosen as an best solution by system-level experiences. And vehicle tests were done for the cabin warm-up performance and power consumption comparison, in the real electric vehicle. Finally we could find out the possibilities for developing the cold climate heat pump (CCHP) for future electric vehicle without high cost and high capacity additional heater.

Keywords: heating performance, heat pump, electric vehicle, vapor injection, cold climate, CCHP, COP

Student Identification Number: 2010-30790

Contents

List of Tables

List of Figures

Nomenclature

A	area of chamber [m^2]
C_p	specific heat [kJ $K^{-1}kg^{-1}$]
C_d	flow coefficient [kJ kg^{-1} K^{-1}]
Comp	compressor
COP	coefficient of performance
CCHP	cold climate heat pump
EV	electric vehicle
HVAC	heating, ventilation and air-conditioning
IHX	internal heat exchanger
NTU	the number of transfer unit
ODAT	outlet discharge air temperature at condenser
CCHP	cold climate heat pump
P	pressure [kPa]
$\dot{Q}$	heating or cooling capacity [kW]
R	gas constant [kJ K^{-1} kg^{-1}]
T	temperature [°C]
V	volume [m^3]
$\dot{W}$	work [kW]
f	compressor rotational frequency

h specific enthalpy [kJ kg^{-1}], height of scroll [mm]

k specific heat ratio

m mass [kg]

$\dot{m}$ mass flow rate [kg s^{-1}]

$\dot{q}$ specific cooling capacity [kW kg^{-1}]

r radius [mm]

t width of scroll wrap [mm]

v specific volume [m^3 kg^{-1}]

$\dot{w}$ specific work [kW kg^{-1}]

Greek letters

Φ orbiting angle [radian]

α starting angle [degree]

β rotating angle in PMP design [degree]

η efficiency

θ rotating angle of involute [degree]

ε effectiveness of a heat exchanger, orbiting radius [mm]

υ specific volume [m^3 kg^{-1}]

Subscripts

A	point A
comp	compressor
dis	discharge port
e	evaporator
c	condenser
ihx	internal heat exchanger
ev	expansion valve
eev	electronic expansion valve
r	refrigerant
a	air
i	inlet
o	outlet
inj	injection
amb	ambient
sc	subcool
sh	superheat
mech	mechanical
isen	isentropic
h	high pressure side

ave	average
cons	consumption
hp	heat pump
PTC	electric PTC(positive temperature coefficient) heater
l	low pressure side
1	upper stream, divided section 1
2	down stream, divided section 2
3	divided section 3
4	divided section 4
5	divided section 5
6	divided section 6

Chapter 1. Introduction

1.1 Background

In recent years, electric vehicles (EVs) are getting more and more popular because the fossil fuel is insufficient and emission regulation is getting strict. And lots of car makers are developing and producing the electric vehicles. However EVs are not prevailed for the public especially due to short driving range relative to internal combustion engine (ICE) vehicle. One challenge that such a short driving range EVs are facing with is the cabin heating. Unlike ICE driven vehicles, EVs don't have sufficient waste heat for cabin heating because of high efficient energy conversion efficiency. A general way to supply heat for EV cabin is to utilize the electric heater, usually called PTC (Positive temperature coefficient) heater, which uses the electricity stored in the battery with drive motor. The capacity of electricity in the electric vehicle battery is not so sufficient that the vehicle is lack of the electric energy for driving mileage when the additional electric heater like PTC heater use the electric power. In short, the electric heater efficiency is very important issue and the power reduction of electric heater is needed for the EV driving mileage because the vehicle shares the electric power with electric heater. Although PTC heater usually has almost 100% first law efficiency, their second law efficiency is very low. For EV with only PTC heater, driving range decrease drastically when PTC heater is turned on. Therefore efficient heat pump is an alternative way to provide comfort cabin heating with less electric

energy consumption, and we investigated to develop the advanced heat pump system for future EVs.

1.2 Literature review

EVs have been developed for a long time. Recently, mass production EVs were developed by various car makers. Here we are researching the cabin heating system installed for various EVs.

1.2.1 EVs with heat pump system

Although heat pump system has benefits for high efficiency, lots of early EVs were used only PTC heater for cabin heating like the mitsubishu iMEV and 1st generation Nissan Leaf. When the customers complained a lot about the driving range reduction with heating, heat pump system was starting to be installed. 2nd generation Leaf and Renault ZOE are the first mass produced EVs to use a heat pump. Kia Soul EV is the EV to use an advanced heat pump which can also recover waste heat from electrical systems.

1.2.2 Heat pump studies for vehicles

For a few decades, researches on heat pump for vehicles has been conducted and published. In 2000, a transcritical CO_2 heat pump prototype was built and studied in the Air Conditioning and Refrigeration Center (ACRC). It says that the heating capacity was not significantly reduced even in very low ambient temperature, and warm-up characteristics was also investigated (*Griannavola and Hrnjak*, 2000). In 2002, Valeo also has studied

with a CO_2 heat pump for various problems including flash fogging, defrosting and integration with engine thermal management (*Hesse et al.*, 2002) It used only one indoor heat exchanger, and there was a risk of flash fogging when we switched from A/C mode to heat pump mode. In 2012, Valeo suggested the heat pump of a direct system and an indirect system with R1234yf , and a modular system with CO_2 (*J.Benouali et al.*, 2012). This study showed that heating capacity drops much faster for R1234yf than that of CO_2 system. The reason was mainly due to very low suction pressure and high pressure ratio of R1234yf system at very low ambient temperature. Denso has developed a CO_2 heat pump system for a fuel cell hybrid vehicle (*Hunemorder et al.*, 2003). It consists of two indoor heat exchanger, one outdoor heat exchanger, an internal heat exchanger, an electric compressor, and several other components. Denso adopted similar heat pump system with R134a for Nissan Leaf. Behr researchers (*Wawzyniak et al.*, 2011) have studied various type heat pump systems including air to air, air to coolant, and coolant to coolant. They said that heating demand increased while potential heating capacity decreased when ambient temperature decreased. At low ambient temperature, the potential heating capacity was not enough to satisfy the heating demand, therefore a PTC heater was necessary for supplementary heat. By comparison of refrigerants with air to air system, R1234yf system is lower by 5% heating capacity and by 10% COP than R134a system. And air to air system provided higher capacity and higher COP than air to coolant system. Delphi developed the unitary HVAC system (*Kowsky et al.*, 2012), which used a compact refrigerant loop, together with a coolant distribution

system to provide both cooling and heating. It can integrate the thermal management of battery and power electronics as well as cabin heating and cooling. Viesteon researched a heat pump to use R134a with 4 way valve to a conventional air conditioning system to switch the flow direction for hybrid EVs and EVs. It could present an amount of 1.5~3kW heating capacity according to the ambient temperature and operating conditions. They reported on a webpage (Visteon heat pump for hybrid and electric vehicles 2012) that it consumes 50% less power than electric heaters and extends electric drive mileage by 30%.

1.2.3 Challenges of EV heat pump

Although automotive heat pump has been studied for several decades as shown in 1.2.2, it is not adopted widely by automotive industry. The reason for it is as follows :

- A lot of cost increase to implement heat pump
- Complexity to package heat pump in the vehicle space
- Performance limitation in cold climate or frosting

Among the above problems, performance degradation in cold climate condition is closely linked with other problems like cost and complex space. For any heat pump system using ambient air as heat source, the potential heating capacity decreases as ambient temperature is getting lower, while heating demand is increasing at the same time. In cold climate condition, heat

pump system needs a PTC heater to provide the difference between heating demand and maximum heat pump heating capacity. Therefore the use of a heat pump cannot eliminate the need for an electric heater, while it makes the system more complex. Inhere usually the difference between heating demand and maximum heat pump heating capacity in cold climate condition is so much that an electric heater should be a high voltage high capacity PTC heater, which costs a lot.

Therefore one of the biggest challenges for future heat pump of EVs should be the cold climate heat pump, which means heat pump with high heating capacity in cold climate condition.

1.3 Objective and scope

The objective of this study is to find out and suggest the solution to improve the heat pump heating capacity in cold climate for EV. Current heat pump system for EV doesn't cover the heating performance in cold climate, and needs an additional electric heater. Although CO_2 heat pump performs better, R134a refrigerant system is undoubtedly the dominant refrigerant for automotive industry and CO_2 system needs higher cost due to higher pressure requirement for components. R134a is getting phased out from automotive industry due to its high global warming potential (GWP), but the alternative refrigerant R1234yf properties are similar to R134a. So this study was restricted to improve the R134a refrigerant heat pump system in cold climate condition. In short, the target for the improved heat pump system can be

described as follows :

- It doesn’t need high voltage PTC heater in cold climate condition
- Equivalent heating performance to conventional vehicle in cold climate condition
- Minimize the electric power consumption for heating in cold climate condition
- Current performance like heating, cooling, NVH, and power consumption should be kept in all other condition except for cold climate condition

At first, in chapter 2, vapor injection heat pump for EV was investigated by system simulation. Vapor injection technology is a common solution for cold climate heating performance improvement in industrial or residential heat pump system, but researches for automotive region was restricted. So

In chapter 3 and 4, we investigated the realistic solution to eliminate the high voltage PTC heater. In chapter 3, we suggested 3 kinds of technical solutions and figured out the performance improvement by system level experiments. Although heat pump system performance was conducted, we should do the vehicle level test to validate the performance considering the cabin thermal load. In chapter 4, we implemented the various cold climate heat pumps (CCHPs) to an real EV, Kia Soul EV, and did a test for heating performance and electric power consumption during heater warm up. And finally a proper CCHP which doesn’t need a high voltage PTC heater, was

suggested for future EVs, and summarized in chapter 5.

Chapter 2. Analysis on the performance of an EV vapor injection heat pump system for cold climate

2.1 Introduction

As a countermeasure against rising oil prices and strict environmental regulations, the highly efficient and eco-friendly features of battery-powered electric vehicle (EV) are getting greater attention. Unlike conventional vehicles, the EV has little waste heat to be removed and supply to the passenger compartment for cabin thermal comfort; thus, heat should be additionally generated from the battery for an EV. Since the operation of heating system significantly affects the EV's fuel economy (maximum driving range), a highly efficient EV heating system is necessary.

The energy efficiency of electric heaters for EV is poor, in general. As an alternative, an air-source heat pump system has been introduced in the automotive industry (*Hosz et al.*, 2006 ; *Tamura et al*., 2005). The air-source heat pump system is economical because the system can provide both heating and cooling. However, the performance of the air-source heat pump system is poor at very low ambient temperatures due to a reduction in refrigerant mass flow rate. As a result, the operation of an air-source heat pump system is restricted to mildly cold conditions. For this reason, the performance of EV heat pump systems in cold weather conditions must be improved.

Several technologies, such as cascade cycle, injection cycle and method of using additional heat have been studied for heat pump to improve the heating performance at low ambient temperatures. Among them, a technique of injecting vapor refrigerant injection into compressors (vapor injection technique) has been studied actively in recent years (*Heo et al.*,2010 ; *Aikins et al.*, 2013 ; *Roh et al.*,2014 *; Roh et al.*,2015 ; *Xu et al*.,2011). However, most of the studies have targeted residential heat pump systems and studies on automotive heat pump systems are limited. A heat pump system for a vehicle differs from residential heat pump systems in many ways. A vehicle can move around, so it experiences a wide range of weather conditions. Most importantly, a residential heat pump system's configuration and size, refrigerant, and operational conditions are not similar to those of the automotive heat pump system.

This paper investigates the characteristics on non-injection EV heat pump system by experiment, and predicts the heating performance of an EV vapor injection heat pump system using an electric scroll compressor. To evaluate the system performance under cold conditions, the performance of a non-injection heat pump system was compared theoretically with that of a vapor injection heat pump. Using thermodynamic theories with a real-size scroll compressor geometry, the vapor injection technique was simulated and the efficiency data were used for the other important components. Finally the model was validated with experimental data. The simulation conditions reflected the operational conditions of an EV heat pump at cold ambient temperatures.

The most distinguishable points of a vehicle heat pump system from a residential heat pump system are the consideration of outlet discharge air temperature at condenser (ODAT) and the same air inlet temperature for condenser and evaporator. In this aspect of view, the heat pump system applied to an EV shows its own peculiar characteristics through the investigations and this study provides the basic performance data for the vapor injection heat pump for an EV application.

2.2 Heat pump system for EV

To evaluate the performance of EV vapor injection heat pump system, an EV vapor injection heat pump system was modeled and calculation was performed considering operating condition of EV heat pump. Also, we tested and analyzed a baseline (non-injection air source) EV heat pump system that has the function and dimensions of an automotive HVAC system.

2.2.1 Baseline EV heat pump concept integrated with cooling system

A baseline (non-injection air source) heat pump system of EV was integrated with a cooling system including R134a refrigerant. The EV heat pump system can replace a conventional coolant using heating system. To understand the detailed EV heat pump configuration, the automotive HVAC functions have to be understood and general automotive HVAC's functions with the cooling and heating system are as follows:

- Passenger thermal comfort (heating in winter, cooling in summer),
- Demisting/defrosting the windshield for safe driving,
- Dehumidifying the cabin for passenger thermal comfort, and
- Ventilation for indoor air quality (IAQ).

Among these functions, demisting or defrosting a windshield is a unique function of a automotive HVAC system. For this function and comfortable IAQ, fresh ambient air is usually blown into the cabin (indoor) in the winter, which is a very different operating condition from a residential heat pump system. Sometimes, simultaneous cooling and heating operation is required for an EV heat pump system (i.e., the automotive heat pump requires two separate indoor heat exchangers one of which functions as an evaporator and the other functions as a condenser). Regarding such functions, the indoor condenser should perform the function of original automotive HVAC's coolant heater core and the size of the indoor condenser should be similar to the original heater core. Because the compact package is very important for a vehicle, an outdoor heat exchanger is used as both evaporator and condenser for the respective appropriate mode. Conventional EV heat pump configurations with these design considerations are shown in Figure 2.1a. To change the refrigerant flow for cooling and heating modes, three additional two-way valves have been added to a conventional EV heat pump system. The EV has an electric scroll compressor, and the specification details are shown in Table 2.1.

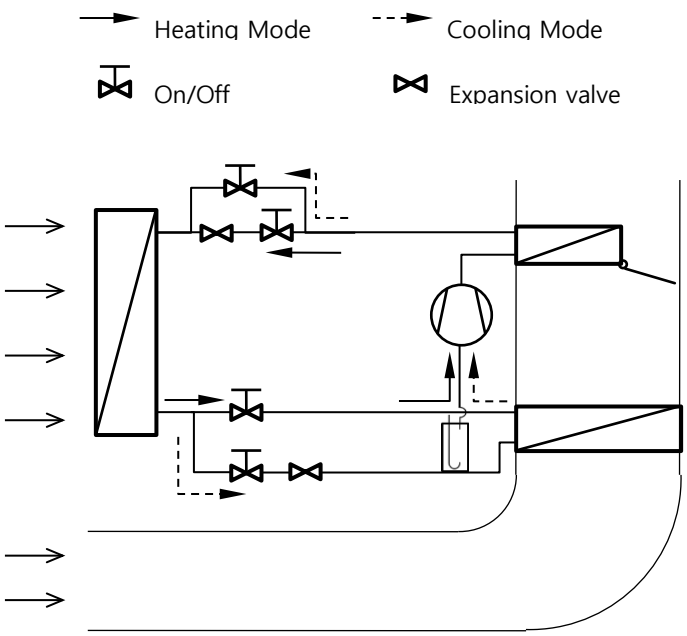

(a)

Figure 2.1 Schematics of
(a) non-injection type heat pump system, and
(b) vapor injection type heat pump system for electric vehicle

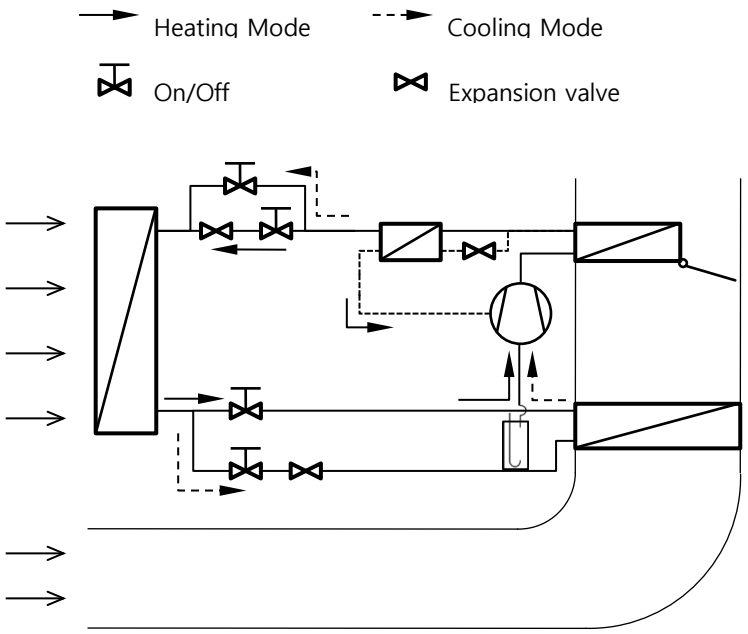

(b)

Figure 2.1 Schematics of
(a) non-injection type heat pump system, and
(b) vapor injection type heat pump system for electric vehicle (continued)

Table 2.1 EV heat pump system specification

Component	Type	Specification
Compressor	Electric scroll compressor	High voltage, 5 kW capacity
Outdoor Evaporator/ Condenser	Air to refrigerant	W570 mm × H400 mm × D20 mm
Indoor Condenser	Air to refrigerant	W200 mm × H180 mm × D27 mm
Indoor Evaporator	Air to refrigerant	W260 mm × H250 mm × D45 mm

2.2.2 Vapor injection heat pump for EV

In this study, we considered an internal heat exchanger (IHX) type vapor injection heat pump system because of the relative easiness for the delicate refrigerant flow control compared with flash tank type vapor injection heat pump system (Roh et al.,2014;Xu et al.,2011). The IHX type vapor injection system needs additional parts; an additional heat exchanger, an electric expansion valve (EEV) to control the flow of injection refrigerant, and an injection compressor. These additional components can be incorporated with the conventional EV heat pump system in an outdoor space, usually called the engine room. In this study, we only focus on the heating performance and deal with the heating mode for automotive HVAC. In heating mode, the EEV controls the refrigerant flow through the IHX, thereby making the refrigerant that has passed through the indoor condenser possible to be used as heat recovery medium. The injected refrigerant should be fully vaporized for compressor protection and the EEV controls the superheat by delicately regulating the injected refrigerant mass flow. The IHX, Injection Compressor and dashed pipe line in Figure 2.1b are the additional parts of the vapor injection heat pump system.

2.3 Analytical model of vapor injection heat pump system

3.2.1 Geometry-based injection scroll compressor model

As heat pump system analysis is conducted with vapor injection, the injected conditions and the situations inside of the scroll compressor should be investigated. Therefore scroll compressor modeling has to be conducted prior to the overall system analysis. An injection scroll compressor is only different from baseline (non-injection) scroll compressor because of its injection hole. Some researchers simplified the scroll compressor model (Winandy et al.,2002;Wang, 2008;Choi et al.,2012) and analyzed the heat pump system. However to model the injection hole, scroll compressor modeling considering the geometric variables may be more effective. Many researchers have established the scroll compressor modeling considering the geometric variables. Hirano (1990) studied the scroll compressor geometry and designed the PMP shape which has thick scroll wraps in middle of the part. Zhenquan (1992) suggested the equations of PMP shape design and Kim (1998) and Park (2002) developed the governing equations for the scroll compressor modeling. In this study, the main purpose of detailed compressor simulation model is to consider injection effect. To accomplish this, a geometry-based thermodynamic approach was applied following a formulated model of the automotive scroll compressor (1998), and to consider the injection process, injection hole area was calculated using graphical method

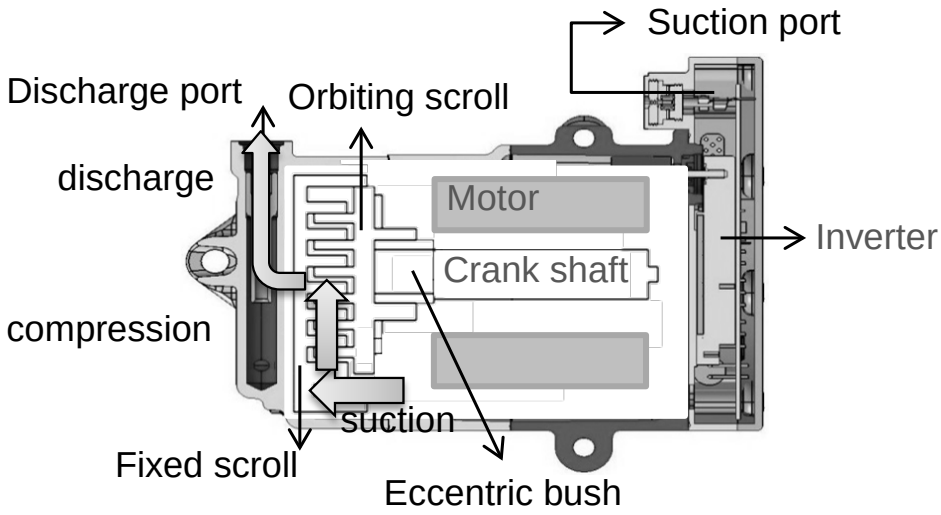

(a)

Figure 2.2 Electric scroll compressors for electric vehicle,
(a) Conventional type, and
(b) vapor injection type (Continued)

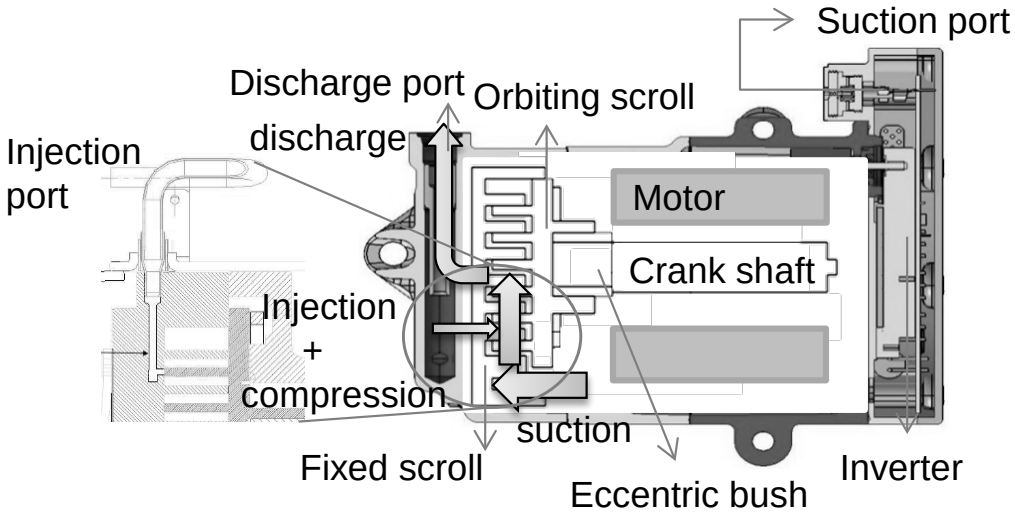

(b)

Figure 2.2 Electric scroll compressors for electric vehicle,
(a) Conventional type, and
(b) vapor injection type

and interpolation. Heat transfer, oil effects, leakage between the scroll lap and clearance, gravitational force and kinetic energy were ignored in compressor calculation process. Instead of considering them, experimental compressor overall efficiency (η_{comp}) was used implicitly for modeling compressor.

$$W_{comp} = \eta_{comp} \times \Delta h_{comp} \qquad (\eta_{comp} = \eta_{motor} \times \eta_{inverter} \times \eta_{mech} \times \eta_{isen}) \tag{1}$$

Governing equations are derived from a mass balance equation and energy conservation equation (Eqs. 2 and 3) for each process (suction, compression, and discharge process) as many researchers have done [5, 17]. Vapor refrigerant injection was modeled using the suction process.

$$\frac{dm}{d\phi} = \sum \frac{dm_i}{d\phi} - \sum \frac{dm_o}{d\phi} \tag{2}$$

$$\dot{Q} + \sum m_i h_i = \frac{d(mu)}{dt} + \sum m_o h_o + \dot{W} \tag{3}$$

$$\dot{W} = P\left(m\frac{dv}{dt} + v\frac{dm}{dt}\right) \tag{4}$$

For a given control volume, the simultaneous differential equations of pressure (P), temperature (T), and mass (m) with respect to the orbiting angle were derived from governing equations (Eqs. 2,3), as follows.

In the suction process,

$$\frac{dT}{d\phi}=\frac{\sum\left(h_i-h\right)\frac{dm_i}{d\phi}-\left(\frac{dV}{d\phi}-\upsilon\cdot\frac{dm}{d\phi}\right)\left(\left.\frac{\partial h}{\partial \upsilon}\right]_T-\upsilon\cdot\left.\frac{\partial P}{\partial \upsilon}\right]_T\right)}{m\left(\left.\frac{\partial h}{\partial T}\right]_\upsilon-\upsilon\cdot\left.\frac{\partial P}{\partial T}\right]_\upsilon\right)} \tag{5}$$

$$\frac{dm}{d\phi}=\frac{C_d\cdot A\cdot P_1}{2\pi f}\cdot\sqrt{\left(\frac{2k}{(k-1)RT_1}\right)\left\{\left(\frac{P_2}{P_1}\right)^{\frac{2}{k}}-\left(\frac{P_2}{P_1}\right)^{\frac{k+1}{k}}\right\}}$$

$$\left(\ when\quad \frac{P_2}{P_1}>\left(\frac{2}{k+1}\right)^{\frac{k}{k-1}}\ \right) \tag{6}$$

$$\frac{dm}{d\phi}=\frac{C_d\cdot A\cdot P_1}{2\pi f}\cdot\sqrt{\left(\frac{k}{RT_1}\right)\left\{\left(\frac{2}{k+1}\right)^{\frac{k+1}{k-1}}\right\}}$$

$$\left(\ when\quad \frac{P_2}{P_1}\le\left(\frac{2}{k+1}\right)^{\frac{k}{k-1}}\ \right) \tag{7}$$

In the compression process,

$$\frac{dT}{d\phi}=\frac{\left(\upsilon\cdot\frac{dm}{d\phi}-\frac{dV}{d\phi}\right)\left(\frac{\partial h}{\partial \upsilon}\right]_T-\upsilon\cdot\frac{\partial P}{\partial \upsilon}\Big]_T\Big)}{m\left(\frac{\partial h}{\partial T}\right]_\upsilon-\upsilon\cdot\frac{\partial P}{\partial T}\Big]_\upsilon\Big)} \tag{8}$$

In the discharge process,

$$\frac{dT}{d\phi}=\frac{\sum\left(h-h_o\right)\frac{dm_o}{d\phi}-\left(\frac{dV}{d\phi}-\upsilon\cdot\frac{dm}{d\phi}\right)\left(\frac{\partial h}{\partial \upsilon}\right]_T-\upsilon\cdot\frac{\partial P}{\partial \upsilon}\Big]_T\Big)}{m\left(\frac{\partial h}{\partial T}\right]_\upsilon-\upsilon\cdot\frac{\partial P}{\partial T}\Big]_\upsilon\Big)} \tag{9}$$

$$\frac{dm}{d\phi}=\frac{C_d\cdot A\cdot P_1}{2\pi f}\cdot\sqrt{\left(\frac{k}{RT_1}\right)\left\{\left(\frac{2}{k+1}\right)^{\frac{k+1}{k-1}}\right\}}$$

$$\left(\ when\quad \frac{P_2}{P_1}\le\left(\frac{2}{k+1}\right)^{\frac{k}{k-1}}\right) \tag{10}$$

$$\frac{dm}{d\phi}=\frac{C_d\cdot A\cdot P_1}{2\pi f}\cdot\sqrt{\left(\frac{2k}{(k-1)RT_1}\right)\left\{\left(\frac{P_2}{P_1}\right)^{\frac{2}{k}}-\left(\frac{P_2}{P_1}\right)^{\frac{k+1}{k}}\right\}}$$

$$\left(\ when\quad \frac{P_2}{P_1}>\left(\frac{2}{k+1}\right)^{\frac{k}{k-1}}\right) \tag{11}$$

Injection hole was assumed to be located at 240° at which refrigerant mass flow rate increase can be maximized. And injection process was included in this model by following the suction process. Basically, the formulas were established corresponding to time and after then it was changed to be correspond to introducing angular velocity. d/dφ means the change of properties corresponds to the small change of orbiting angle of the orbiting scroll.

We also assumed that properties of the working fluid inside of a control volume were constant and the refrigerant was R134a. This study is trying to provide system performance with R134a (GWP of 1300, Myhre et al.,2013), however, the results can be applied to the alternative low GWP refrigerant R1234yf (GWP less than 1,Myhre et al.,2013) system because R1234yf has the similar thermal properties with R134a. This injection scroll compressor model needs several input conditions like the pressure on the suction, injection and discharge and superheat on suction and injection, which were presented by the heat pump system analysis. Using the given initial values the refrigerant mass flow rate, and discharge temperature, from which we can calculate all the enthalpy, can be calculated.

The volume equation in each step is given in Appendix. Geometric parameters used in the volume equations are shown in Table 2.2.

2.3.2 Other components (heat exchanger, expansion valve) model

We applied the simple model for the heat exchanger and expansion valve.

Table 2.2 Geometric parameters of the scroll compressor

Parameters	Value	Scroll design figure
Scroll height: h (mm)	25	
Scroll thickness: t (mm)	4	
Basic circle radius: r (mm)	3.4	
Orbiting radius: ε (mm)	6.8	
Starting angle of outer involute: αo (mm)	68.4	
Starting angle of inner involute: αi (mm)	0	
Maximum involute angle : θe (°)	945	
Modified angle: γ (°)	112	
Rotating angle: β (°)	14	
Circular arc radius of outer scroll: ro (mm)	3.892	
Circular arc radius of inner scroll : ri (mm)	10.602	
Injection port position (degree)	240	
Injection port radius (mm)	2	

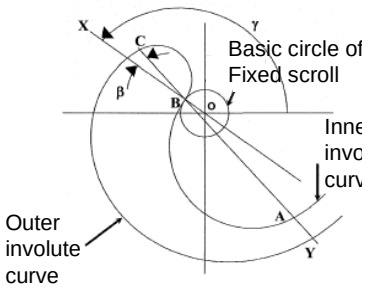

The vapor injection heat pump system shares the heat exchanger with the baseline heat pump system. Air to refrigerant compact heat exchangers were applied for outdoor evaporator and indoor condenser [Table 2.1]. Thus, we can reuse the heat exchangers' performance data for the analysis. Note that the models of these heat exchangers were based on the effectiveness(ε) as the ratio of the actual heat transfer rate for a heat exchanger to the maximum possible heat transfer rate, which originated from the component test results (Eqs. 12 and 13).

$$\dot{Q}_{hx} = \varepsilon \times \dot{Q}_{\max} = \varepsilon \times \dot{m}_a C_{p,a}(T_{\mathrm{r,in}} - T_{a,\mathrm{inlet}}) = \dot{m}_r (h_i - h_o) \tag{12}$$

$$\varepsilon = f(\mathrm{NTU}, \frac{\dot{m}_a C_{p,a}}{\dot{m}_r C_{\mathrm{p,r}}}) \tag{13}$$

Expansion valve was modeled by isenthalpic process, which means the ideal function of an expansion valve is to expand the refrigerant without enthalpy loss. In a throttling, the refrigerant pressure is lowered from a high condensing pressure to a low evaporating pressure. We assumed that the refrigerant flow has no heat loss in the expansion valve.

Internal heat exchanger (IHX) has important role for refrigerant vaporization, which is refrigerant to refrigerant heat exchanger. No heat loss to air was assumed for IXH modeling (isolation to environment, heat transfer

occurs between refrigerant only). The modeling of heat exchange is represented bellows:

$$\dot{Q}_{IHX,h} = (\dot{m}_{ref} - \dot{m}_{ref,inj}) \times (h_{cond.out} - h_{IHX.h}) \quad (14)$$

$$\dot{Q}_{IHX,l} = \dot{m}_{ref,inj} \times (h_{IHX.l} - h_{cond.out}) \quad (15)$$

$$\dot{Q}_{IHX,l} = \dot{Q}_{IHX,\mathrm{h}} \quad (16)$$

The refrigerant discharge temperature of IHX to expansion valve cannot be lower than refrigerant discharge temperature of IHX to compressor, and we assumed the bellows:

$$T_{IHX,\mathrm{l,o}} = T_{IHX,\mathrm{h,o}} \quad (17)$$

We covered only steady state condition, and ignored the accumulator modeling. For simplicity, we also ignored the refrigerant pressure drop modeling for the entire components.

2.3.3 Performance simulation algorithm of the heat pump system

Considering dimensions of a mobile heat pump system, we composed an analytical vapor injection heat pump system by combining the geometry-based injection scroll compressor model and the other components' model. To evaluate the analytical vapor injection heat pump model, we need some inputs and iterations. In an EV heating system, the outlet air temperature influences the passenger thermal comfort directly. To consider the outlet air temperature, first the outlet air temperature was determined, and then others were calculated in the study, like the indoor air volume flow rate. Figure 2.3 shows the flow chart of performance simulation. The performance was predicted as follows:

First, the engineering data and the operating conditions were provided as inputs: geometry and efficiency test data for modeling, subcool and superheat temperature difference, desired outlet air temperature set, operating compressor speed for operating condition and ambient temperature. Then, the refrigerant pressure at each component was assumed and initialized. The refrigerant mass flow rate, pressure and temperature of the cycle have been determined through the subroutine function and refrigerant cycle. Finally, this simulation process was repeated until the superheat temperature of the injection side reached the setting value. To make the iteration converge, Runge-Kutta method was used in the all required processes. The convergency criteria were basically 0.1˚C for the simulation.

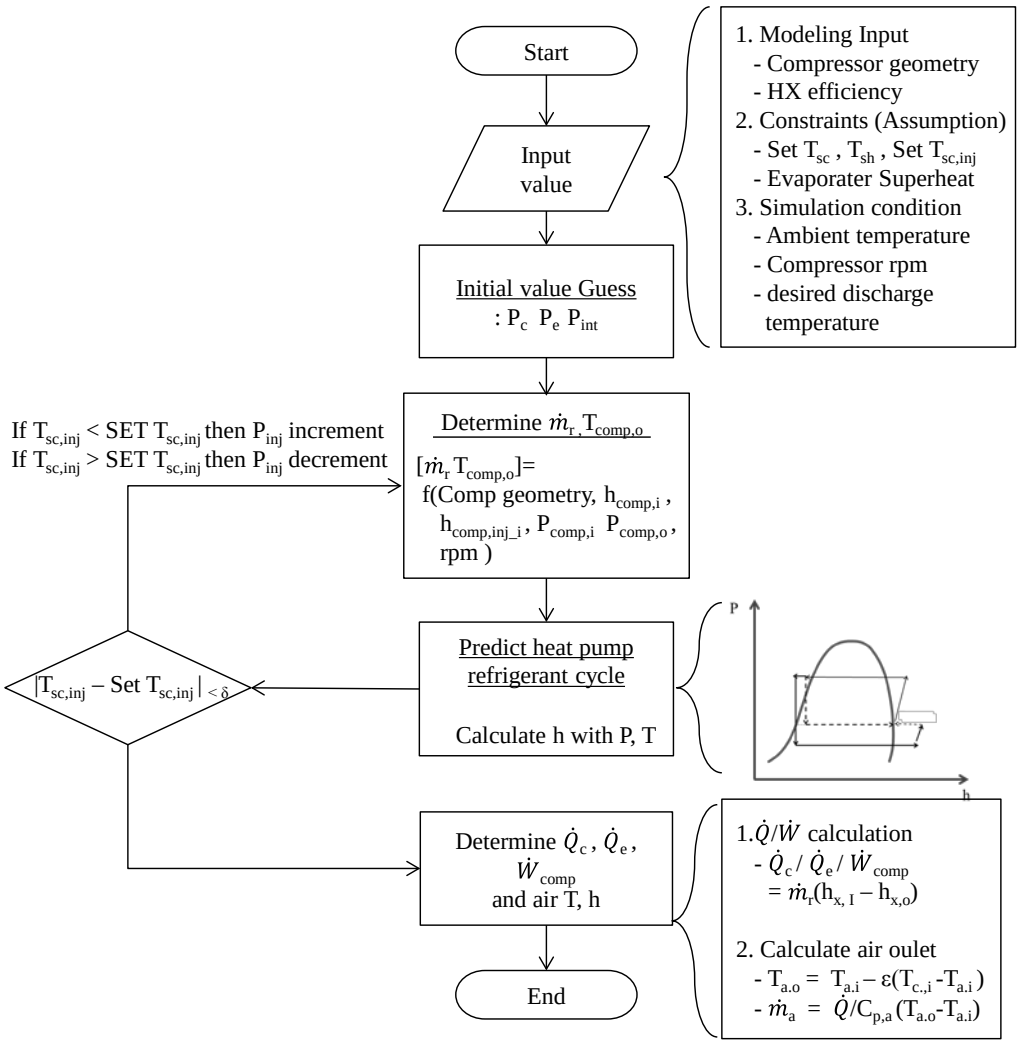

Figure 2.3 Flow chart for heat pump simulation

2.3.4 Validation

The compressor model and the heat pump system simulation program were validated by comparing the predicted results with the experimental data for the non-injection condition at the same operating condition. The scroll compressor without refrigerant injection was tested in a compressor calorimeter according to the ISO 917. The compressor calorimeter consists of two components: a refrigeration system including test section and cooling/heating system to maintain suction and discharge condition. The performance of the compressor without refrigerant injection was measured by varying the pressure ratios from 4 to 8 with 2 intervals at each compressor speed (3000 rpm, 5000 rpm, and 7000 rpm). For compressor model validation, the refrigerant mass flow rates were compared as a function of the compressor operating speed and pressure ratio. The fitting curve slope is 1.04 and the R2 is 0.992. The compressor power consumption was also compared, and the fitting curve slope is 1.11 and the R2 is 0.986. The error band of predicted results for the compressor is less than 20%, and the trend agreed well (Figure 2.4 a, b).

For the heat pump simulation program, the heat pump system without refrigerant injection was tested in an HVAC system calorimeter according to the SAE J2765. The system calorimeter consists of two climate control chambers including cooling/heating system to maintain the climatic test condition. We collected the experimental data from both the air side and the refrigerant side, but air side temperature distribution was less uniform, so we

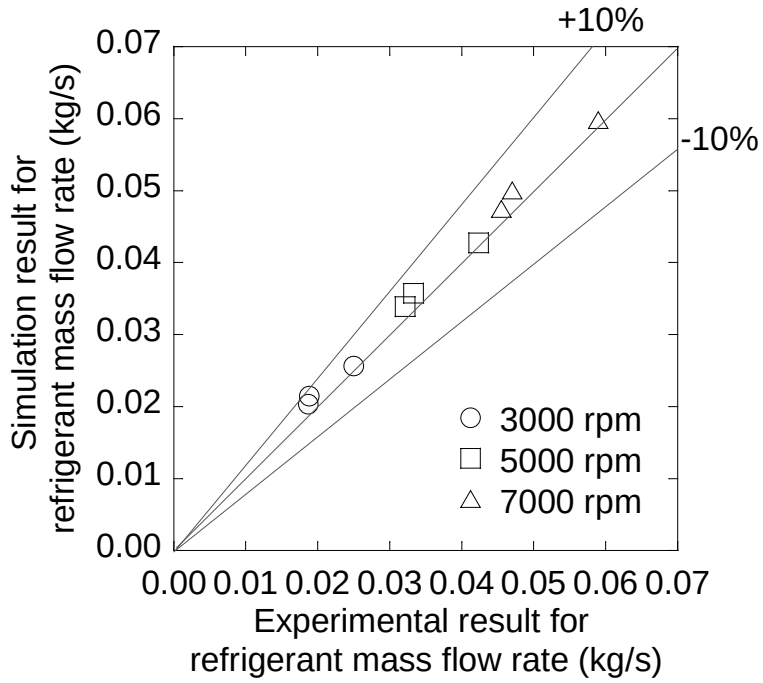

(a)

Figure 2.4 Comparison between experiment and simulation for
(a) refrigerant mass flow rate, and
(b) compressor power consumption
(pressure ratio 4, 6, 8 at 3000 rpm, 5000 rpm, and 7000 rpm respectively)

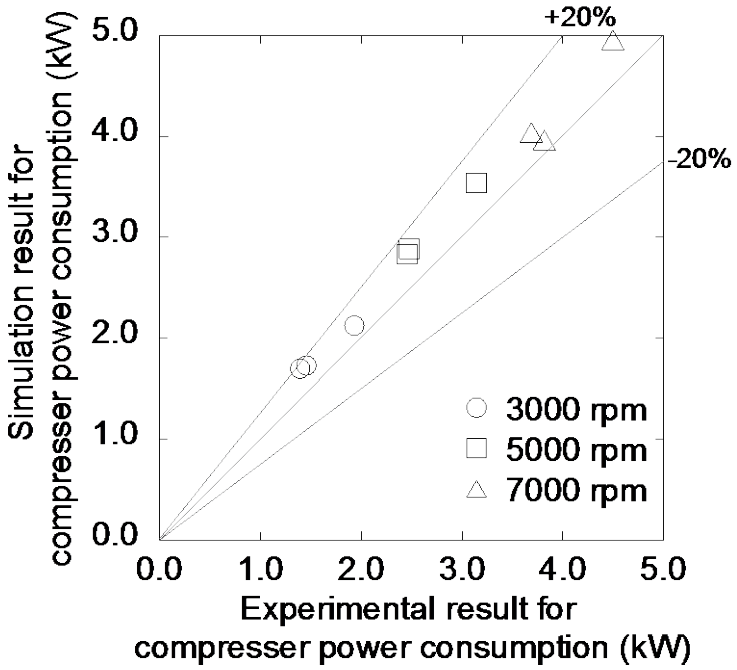

(b)

Figure 2.4 Comparison between experiment and simulation for
(a) refrigerant mass flow rate, and
(b) compressor power consumption
(pressure ratio 4, 6, 8 at 3000 rpm, 5000 rpm, and 7000 rpm respectively) (Continued)

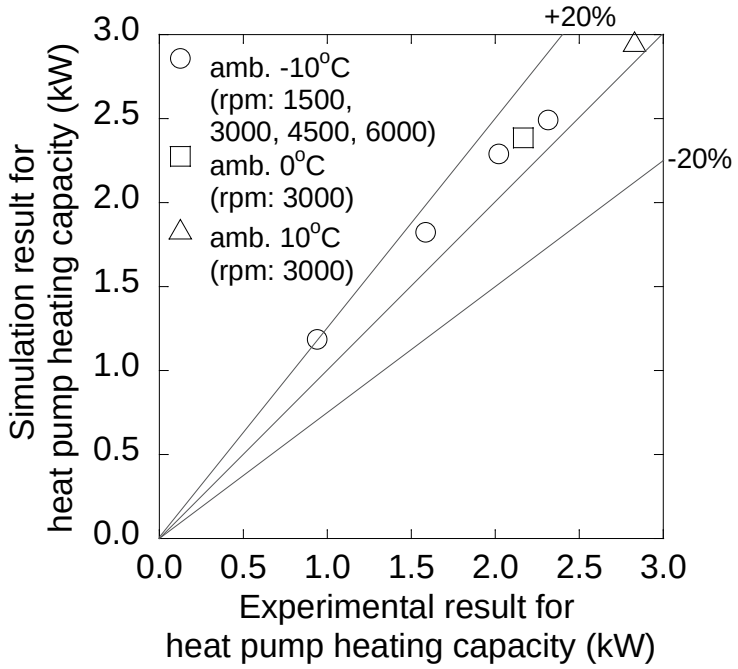

Figure 2.5 Comparison between experiment and simulation for non-injection type heat pump heating capacity

Table 2.3 Heat pump experimental condition for validation

Amb. Temp. (℃)	Air flow rate to indoor HX ($m^3 h^{-1}$)	Air flow rate to outdoor HX ($m^3 h^{-1}$)	Comp. speed (RPM)	Comments
10	300	1450	3000	Air temp to HX is equal to amb. temp
0	300	1450	1500/ 3000	
-10	300	1450	4500/ 6000	

used the refrigerant side data. At the inlet and outlet of the each heat exchanger, the compressor, and outlet of the expansion valve, K-type thermocouples and pressure transducers were used to measure the temperature and pressure. Refrigerant mass flow rate was measured by Coriolis type mass flow meter by Oval (Ultra Mass MK-2). The heating performance of the EV heat pump without refrigerant injection was tested by several conditions (Table 2.3). The heating capacities were compared as a function of the compressor operating speed and ambient temperature. The fitting curve slope is 1.13 and the R2 is 0.986. The error band of predicted results for the heat pump heating performance is almost less than 20%, and the trend agreed well. All simulation results of the compressor model and heat pump system model tend to be higher than experimental results. However, Figure 2.4 and 2.5 shows good agreement and same result pattern between the simulation and experiment.

2.4 Results and discussions

2.4.1 Experimental study of the EV baseline (non-injection) heat pump system

To consider the performance characteristics of the baseline (non-injection) EV heat pump system according to the ambient temperature, we analyzed the experiment data varying the ambient temperature at the several operating conditions as shown table 2.3. The compressor operated at 3000rpm and an air flow rate through the indoor heat exchanger was set on 300 m3h-1 and an air

flow rate through the outdoor heat exchanger was set on 1450 m3h-1. COPs are calculated only considering heat capacity and compressor power consumption.

Figure 2.6a shows the quantitative effect of ambient temperature variation on the heating capacity and coefficient of performance (COP). As the ambient temperature decreased, the heating capacity decreased. The low ambient temperature causes the low refrigerant pressure, which increases the specific volume drastically and also reduces the refrigerant mass flow rate. The reduced refrigerant mass flow rate reduces the heating capacity. However the COP increased as the ambient temperature decreased, which is different from the previous study (Wang et al.,2008). One should note that as outdoor temperature decreases, indoor temperature also decreases resulting in the decrease of compressor work (Figure 2.6b) and the pressure ratio (Figure 2.6c). As these effects are combined, COP can be increased.

This is one of the unique characteristics of automotive heat pump system. Usually the residential HVAC uses the recirculated air for the air supply to indoor condenser, while the automotive HVAC uses the fresh ambient air as mentioned in section 2.2.1. It can lead the different pressure ratio pattern according to the ambient temperature. As indoor and outdoor temperature decreases, specific volume of refrigerant at suction port becomes larger and the circulating refrigerant flow decreases. As a result, condenser pressure becomes lower and more specific enthalpy change of refrigerant occurs in the heat exchangers respectively. In this reason, the irreversibility in heat exchanger process is reduced and COP can be increased. In conclusion, EV

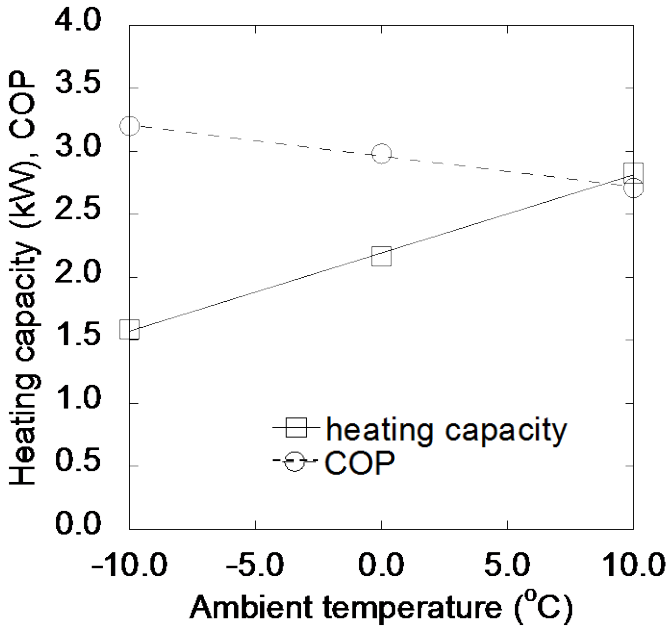

(a)

Figure 2.6 Experimental results of EV non-injection type (baseline) heat pump as a function of ambient temperature on
(a) heating capacity and COP,
(b) compressor power consumption,
(c) refrigerant pressure ratio,
(d) outlet discharge air temperature at condenser.

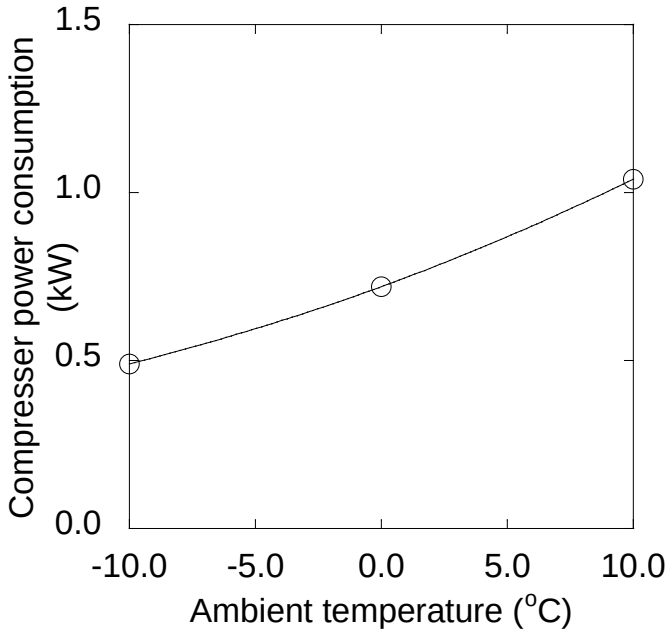

(b)

Figure 2.6 Experimental results of EV non-injection type (baseline) heat pump as a function of ambient temperature on
(a) heating capacity and COP,
(b) compressor power consumption,
(c) refrigerant pressure ratio,
(d) outlet discharge air temperature at condenser.
(Continued)

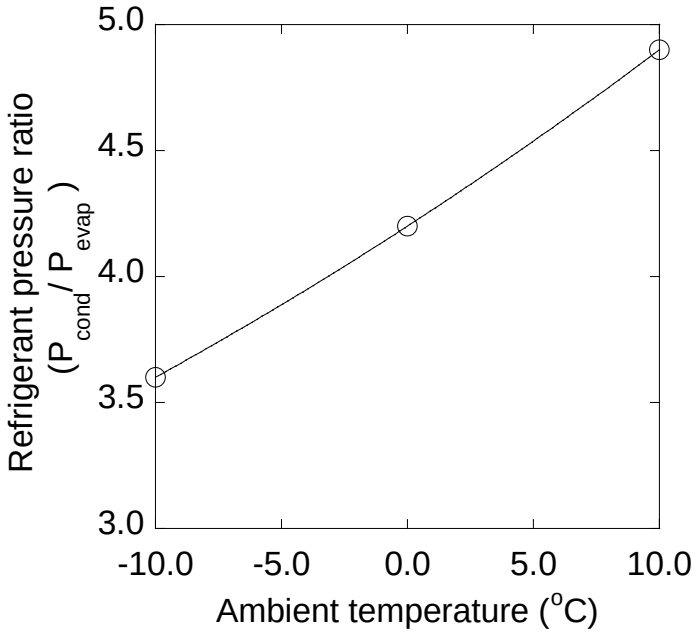

(c)

Figure 2.6 Experimental results of EV non-injection type (baseline) heat pump as a function of ambient temperature on
(a) heating capacity and COP,
(b) compressor power consumption,
(c) refrigerant pressure ratio,
(d) outlet discharge air temperature at condenser.
(Continued)

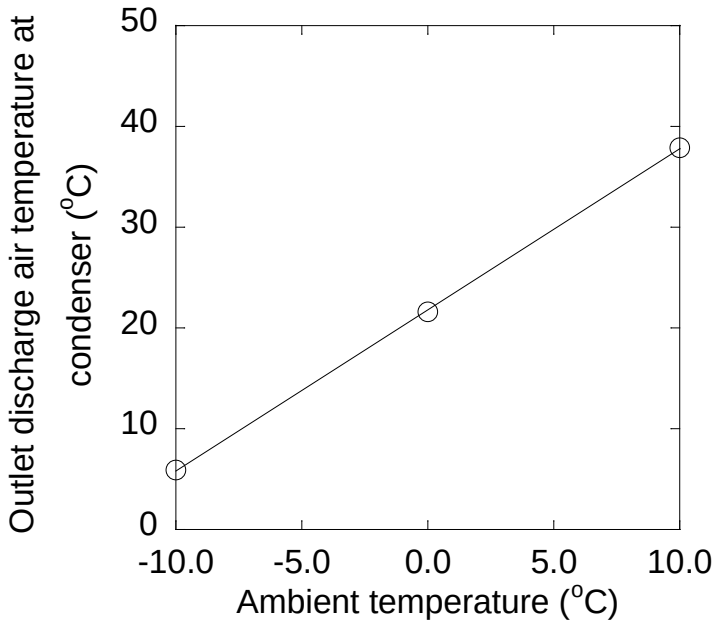

(d)

Figure 2.6 Experimental results of EV non-injection type (baseline) heat pump as a function of ambient temperature on
(a) heating capacity and COP,
(b) compressor power consumption,
(c) refrigerant pressure ratio,
(d) outlet discharge air temperature at condenser.
(Continued)

heat pump system needs the heating capacity improvement more than the COP for the low ambient condition. Also, the heating capacity reduction leads to the decrease of the outlet discharge air temperature at condenser (ODAT), which is closely related to the passenger's comfort feeling (Figure 2.6d). Therefore ODAT is also important for the EV heat pump system development.

2.4.2 Analytic study of the EV vapor injection heat pump system in cold condition

Section 2.4.1 states that improving the heat pump system in terms of heating capacity and outlet air temperature under cold ambient conditions is important. Considering the passenger's thermal comfort, ODAT necessarily should be improved with the heating capacity simultaneously. Thus, to consider the effects of the vapor injection heat pump system for passenger thermal comfort, we simulated the baseline and vapor injection heat pump system, varying ODAT and indoor air flow rate at a cold ambient temperature (20°C) at a fixed compressor frequency of 5000rpm. COPs are calculated dividing heat capacity by compressor power consumption.

Figure 2.2.7 compares the simulated results between the baseline heat pump and vapor injection heat pump system when the ODAT varies, which was driven by the different air mass flow rate through the indoor heat exchanger (Figure 2.7d). As the ODAT increases, the heating capacity of the baseline heat pump decreases. In contrast, the heating capacity of the vapor injection heat pump increases. The improvement rate of heating capacity by the vapor injection technique is 14~44%. The improvement rate is higher at

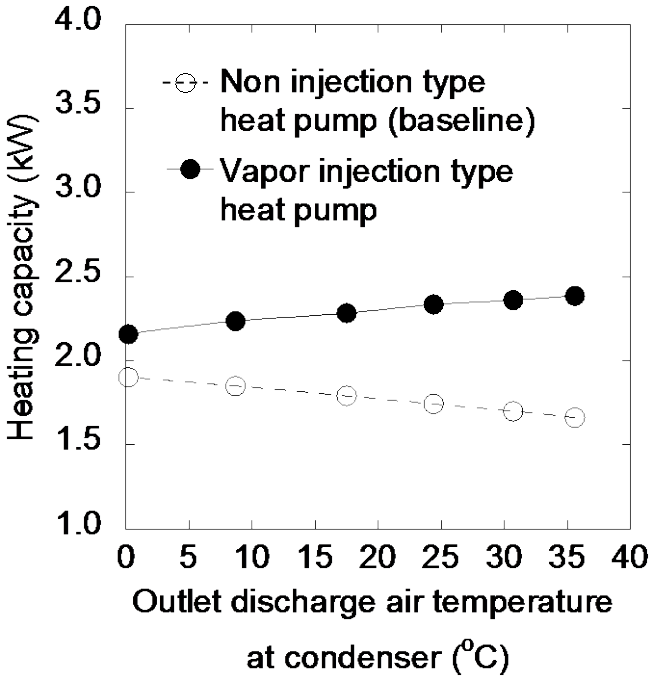

(a)

Figure 2.7 Heat pump performance comparisons between non-injection heat pump and vapor injection heat pump on
(a) heating capacity,
(b) COP,
(c) refrigerant mass flow rate, and
(d) air supply to condenser (compressor speed of 5000rpm and ambient temperature of -20℃).

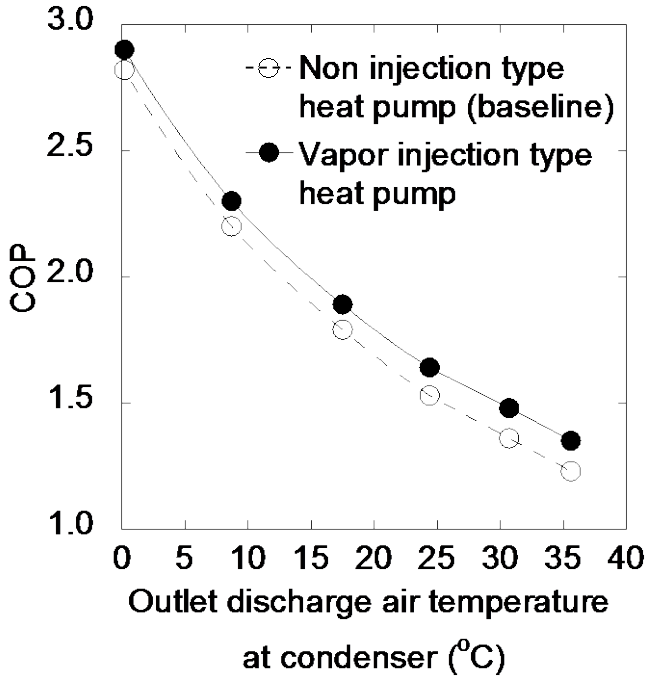

(b)

Figure 2.7 Heat pump performance comparisons between non-injection heat pump and vapor injection heat pump on (a) heating capacity, (b) COP, (c) refrigerant mass flow rate, and (d) air supply to condenser (compressor speed of 5000rpm and ambient temperature of -20℃). (Continued)

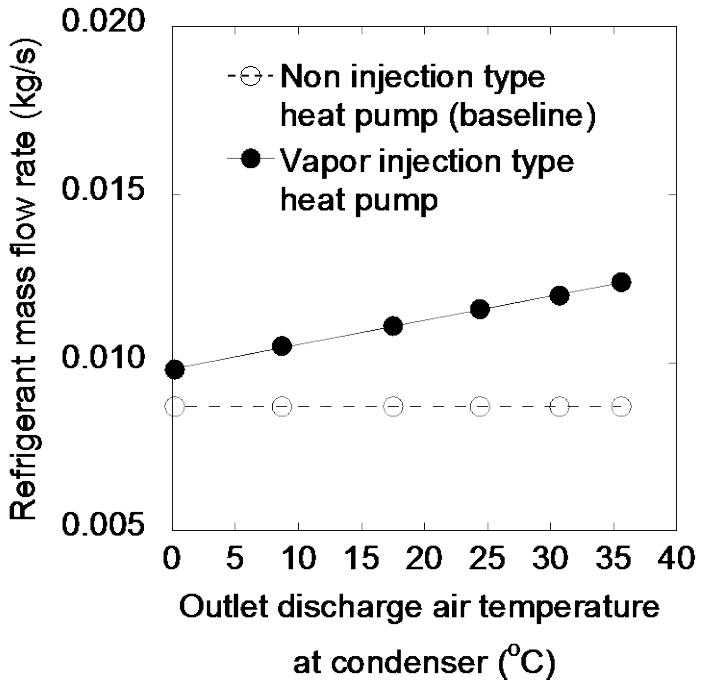

(c)

Figure 2.7 Heat pump performance comparisons between non-injection heat pump and vapor injection heat pump on (a) heating capacity, (b) COP, (c) refrigerant mass flow rate, and (d) air supply to condenser (compressor speed of 5000rpm and ambient temperature of -20℃). (Continued)

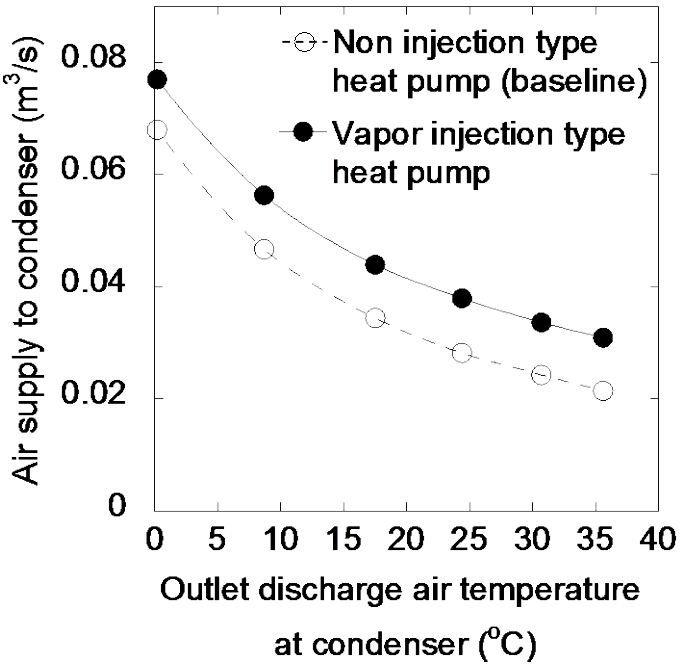

(d)

Figure 2.7 Heat pump performance comparisons between non-injection heat pump and vapor injection heat pump on (a) heating capacity, (b) COP, (c) refrigerant mass flow rate, and (d) air supply to condenser (compressor speed of 5000rpm and ambient temperature of -20℃). (Continued)

an increased ODAT (Figure 2.7a). Even though the COP of the both heat pumps decreases as the ODAT increases, the COP of the vapor injection heat pump is higher than that of the baseline (Figure 2.7b). Figure 2.7c shows the refrigerant mass flow rate of the both heat pumps, which is related to the heating capacity increase. According to the results of Figure 2.7c, the vapor injection technique increases the refrigerant mass flow rate by 13~ 44% as the outlet air temperature increases. It is almost proportional to the increased heating capacity.

From these results, we can summarize two things about the EV vapor injection heat pump system. First, when we want to achieve the same ODAT under cold climatic conditions, the vapor injection heat pump system can give more heating capacity with higher COP performance by increasing the indoor air flow rate. This improvement can be analyzed to be the result of the increased refrigerant mass flow rate. Second, as the ODAT varies for the thermal comfort control under cold climatic conditions, the pattern of heating performance in the each heat pump system is different. With the increased ODAT, the heating capacity of the baseline heat pump system decreased. However, that of the vapor injection heat pump system increased. Both COPs decreased.

As a result, the vapor injection technique may be an appropriate solution for EV heating performance improvement and provide an efficient ODAT increase in cold conditions to achieve passenger thermal comfort control.

To analyze the effects of the vapor injection technique, we compared the energy balance at two ODAT between the baseline heat pump and the vapor

injection heat pump (Table 4.4). Conceptual P-h diagrams based on the simulation results are shown in Figure 2.8.

When the ODAT increased from 0°C to 36°C, the condensing high pressure rose and pressure ratio also increased. Therefore the compressor work increased. Inspite of the more compressor work, the heating capacity decreased from 1.90kW to 1.35kW by 29% with the increased ODAT at the indoor condenser. Because the liquid enthalpy at the refrigerant saturation table increased, and the enthalpy difference in the indoor condenser and outdoor evporator decreased.

However at the same condition, the results of EV vapor injection heat pump system is different. With the increased ODAT from 0°C to 36°C, the heating capacity increased from 2.16 kW to 2.39 kW by 11%. Consequently, at the same ODAT of 36°C, the vapor injection technique increased the refrigerant mass flow rate by 44%, which made the compressor work more and increased internal heat exchange in the internal heat exchanger. This internal heat exchange increased the heat absorption by 214% in the outdoor evaporator. The increased compressor work and heat gain in the outdoor evaporator is the reason why the vapor injection heat pump showed a higher heating performance, by 44%. Comparing the amount of the energy gain in the compressor and evaporator, the energy gain in the evaporator is more than that in the compressor, by 454%. Figure 2.8a,b shows the P-h diagram comparison between the baseline heat pump and vapor injection heat pump with IHX.

Considering the performance of the vapor injection heat pump in the two ODAT of 0°C and 36°C, both the high refrigerant pressure and intermediate

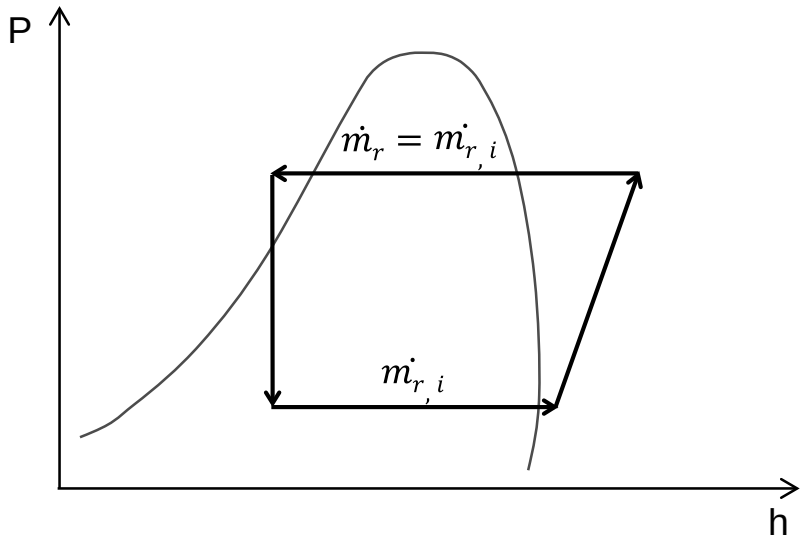

(a)

Figure 2.8 Pressure enthalpy diagram for
(a) non injection type heat pump,
(b) vapor injection type heat pump, and
(c) vapor injection type heat pump with reduced air supply to condenser

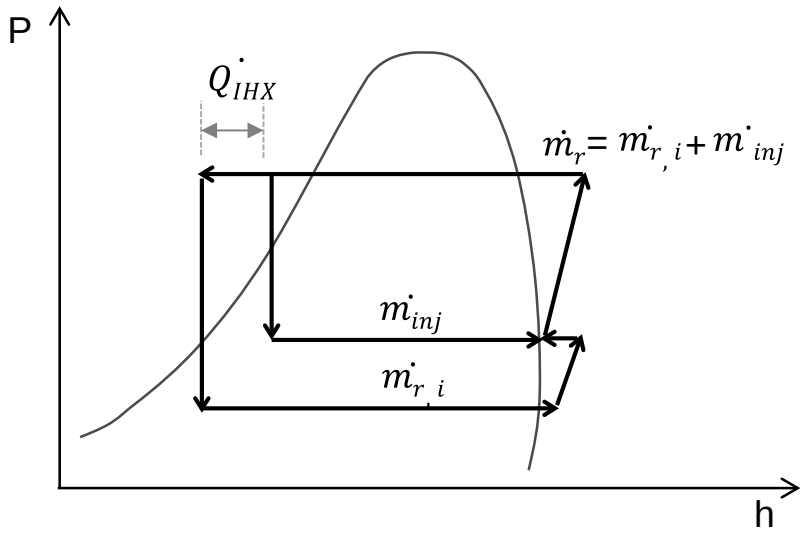

(b)

Figure 2.8 Pressure enthalpy diagram for
(a) non injection type heat pump,
(b) vapor injection type heat pump, and
(c) vapor injection type heat pump with reduced air supply to condenser (Continued)

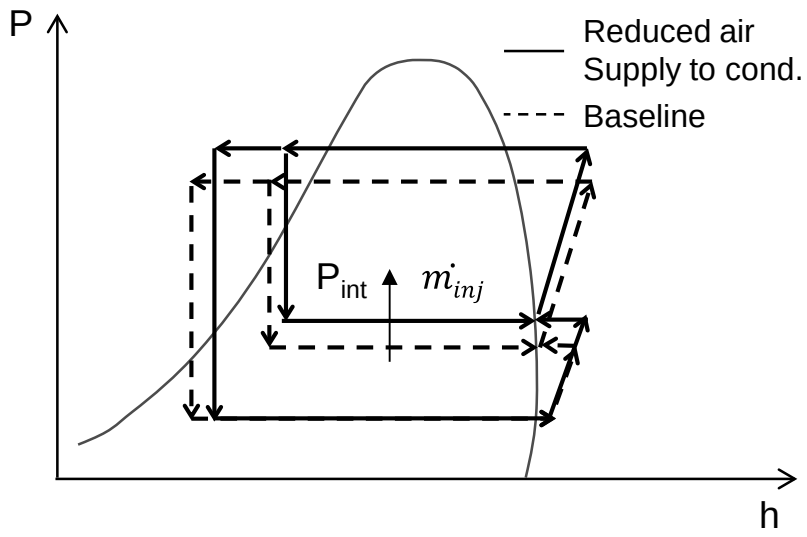

(c)

Figure 2.8 Pressure enthalpy diagram for
(a) non injection type heat pump,
(b) vapor injection type heat pump, and
(c) vapor injection type heat pump with reduced air supply to condenser (Continued)

Table 2.4 Refrigerant energy balance in each component (baseline heat pump and VI heat pump)

	Baseline(non injection)		Vapor injection	
	ODAT 0°C	**ODAT 36°C**	**ODAT 0°C**	**ODAT 36°C**
Compressor (W)	303	608	336	795
Indoor condenser (W)	-1902	-1351	-2159	-2387
Outdoor evaporator (W)	1599	743	1823	1592
IHX to Compressor (W)	-	-	231	533
IHX to expansion valve (W)	-	-	-231	-533

pressure increased at the higher ODAT (Figure 2.8c). The refrigerant mass flow rate at the 36°C ODAT was more than that at the 0°C ODAT, by 31%, which increased the compressor work by 237% and increased internal heat exchange in the internal heat exchanger by 231%. However, with the increased ODAT, the energy gain in the outdoor evaporator decreased by 13%. Totally, compressor work increase was more than the heat gain decrease, so the heating capacity was higher at the higher ODAT, however COP was lower. Thus, the vapor injection heat pump performance, like the heating capacity and COP, varies according to the summation of the compressor work increase and the energy gain in the evaporator, which is influenced by the intermediate refrigerant pressure. In total, the vapor injection heat pump system has the benefit of the heating capacity and COP due to the more heat recovery in the evaporator.

2.4.3 Analytic study of the EV heat pump system optimization in cold condition

In section 2.4.2, we dealt with vapor injection heat pump performance characteristics as we varied the ODAT by changing the HVAC air flow rate. And we can find out that vapor injection technique can improve the heating capacity and COP in cold climate condition, but it still needs additional electric heater. This section will cover the heat pump system redesign and performance optimization by changing the compressor capacity, which is the most important component for deficient refrigerant mass flow rate improvement in cold climate. For the performance simulation, we used the

same model and simulation algorithm except for the compressor scroll height dimension. By changing the scroll height, we could vary the compressor volume capacity. Of course, HVAC air flow rate was maintained by 300 CMH. Other operating conditions were exactly the same as before.

At first, we simulated the performance of non-injection and vapor injection heat pump system according to increased scroll height. Figure 2.9 (a) shows the required compressor capacity increase for the ODAT in cold climate condition. Considering the cabin heating performance and cabin air reuse, the target ODAT may be determined by 35℃. Therefore from Figure 2.9 (a), we can get the required compressor capacity for the cabin heating performance only by heat pump in cold climate. For non-injection heat pump, 3.9 times bigger compressor is necessary, and for vapor injection heat pump, 2.7 times bigger compressor is necessary. If we would like to redesign the heat pump system without additional heater for cold climate, the vapor injection technique can reduce the compressor volume increase, but the compressor should be increased more.

Figure 2.9 (b) shows the heating capacity and COP of heat pump system according to various ODAT. Even though we maintain the HVAC air flow rate, COP decrease as ODAT increase due to refrigerant pressure ratio increase. The COP decrease trend is same for non-injection and vapor injection. The COP of 35℃ ODAT is about half of COP of baseline heat pump. But COP of the vapor injection is better than that of non-injection by 3~10%.

In next step, we tried to optimize the heat pump system considering the power consumption. As we vary the compressor capacity, ODAT also varies.

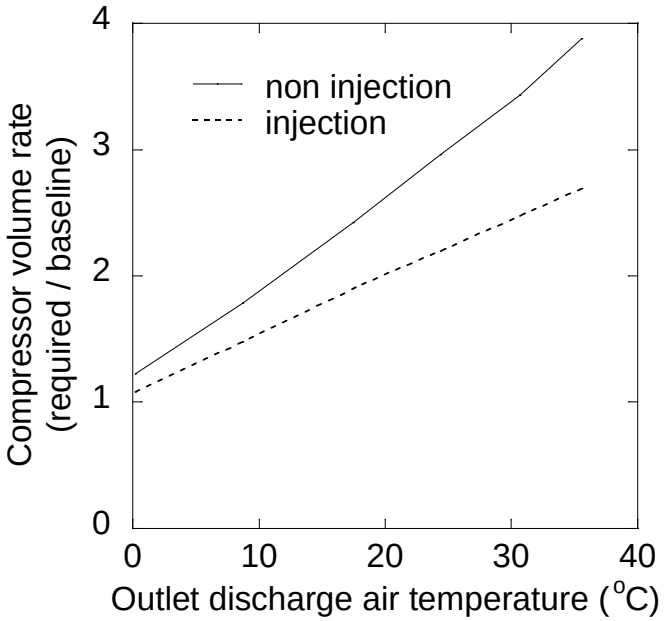

(a)

Figure 2.9 Simulation result according to varying ODAT of heat pump, applying the varying scroll volume of compressor (non-injection and injection)

(a) required compressor volume ratio

(b) COP and heating capacity of heat pump only

(c) Total COP of heat pump and PTC combined

(Continued)

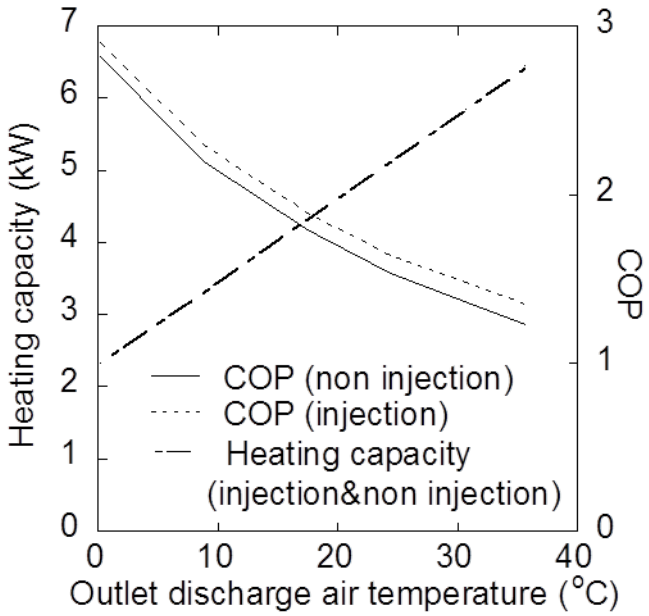

(b)

Figure 2.9 Simulation result according to varying ODAT of heat pump, applying the varying scroll volume of compressor (non-injection and injection)

(a) required compressor volume ratio

(b) COP and heating capacity of heat pump only

(c) Total COP of heat pump and PTC combined

(Continued)

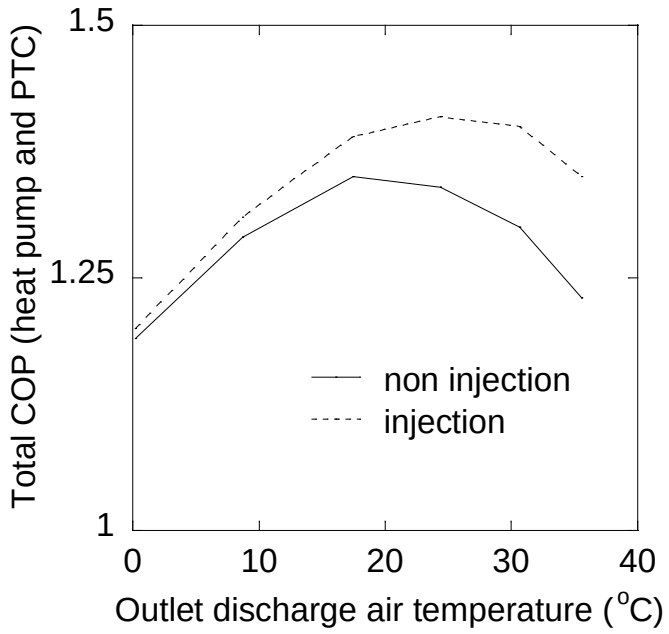

(c)

Figure 2.9 Simulation result according to varying ODAT of heat pump, applying the varying scroll volume of compressor (non-injection and injection)

(a) required compressor volume ratio

(b) COP and heating capacity of heat pump only

(c) Total COP of heat pump and PTC combined

To obtain the target ODAT, we can use the additional PTC heater. When we overcome the deficient heating capacity by PTC heater, we can predict the total COP considering the total power consumption of both system. Figure 2.8 (c) shows the total COP of heat pump and PTC heater combined system according to varying ODAT of the heat pump. From Figure 2.8 (c) there is a optimized combination of compressor increase rate and PTC heater capacity. For non-injection heat pump, 2.4 times compressor and 2kW PTC heater combination has the best COP. The COP benefit for current system is about 13%. For vapor injection heat pump, 2.2 times compressor and 1.3kW PTC heater combination has the best COP. The COP benefit for current system is about 18%.

2.5 Conclusions

In this study, a non-injection heat pump and a vapor injection heat pump system for EV has been modeled. The model included a scroll compressor geometry and test data for EV heat pump components. The EV non-injection heat pump system has also been experimented and studied according to the various ambient temperature condition with EV operational condition. The simulation provided results of the non-injection heat pump and vapor injection heat pump system for a cold ambient temperature with the EV heat pump dimension. An energy balance analysis was also performed to investigate the vapor injection effect on the heat pump performance. Based on the experimental and analytical evidence, the conclusions are summarized as

follows.

(1) In a heat pump of an EV, the heating capacity and outlet air temperature drop with a decreased ambient temperature. Thus, in cold climate conditions, the heat pump system is considered as a supplementary heating system and needs an additional electric heater, which consumes stored electric power, which is why the vapor injection technique should be developed.

(2) Application of the vapor injection technique to an EV heat pump can increase the heating capacity in cold regions. However, the heating capacity improvement rate varies with the ODAT, which can be important for the EV passengers' thermal comfort. The improvement rate was the highest at an increased ODAT, which is a more useful operating condition for the passenger thermal comfort.

(3) The improvement in the vapor injection heat pump performance is due to increased compressor work and the increased heat recovery in the outdoor evaporator, driven by the increased refrigerant mass flow rate. It was induced by the injected vapor refrigerant from the internal heat exchanger.

(4) The vapor injection technique needs a vapor injection compressor and injected vapor refrigerant regeneration components, like an internal heat exchanger and expansion valve. It makes the increase of compressor specific internal energy and causes more heat recovery in the evaporator.

(5) There is an optimized heat pump system for cold climate condition, and vapor injection technique can help minimizing the compressor increase and improving the COP.

Chapter 3. Experiments on the performance improvement of heat pump system for electric vehicle during the cold climate operation

3.1 Introduction

As one of the countermeasures against rising oil price and strict environmental regulations, the highly efficient and eco-friendly features such as a battery-powered electric vehicle (EV) are getting greater attention. Unlike conventional vehicles, during its power generation the EV has little waste heat that can be supplied to the passenger compartment for cabin thermal comfort. Thus heat should be additionally generated by battery of the EV. Because the operation of heating system significantly affects the EV's fuel economy (driving range), a highly efficient EV heating system is necessary.

The energy efficiency of electric heaters for EV is poor in general. As an alternative, an air-source heat pump (ASHP) system has been introduced in the automotive industry (Figure 3.1) (Hosz et al.,2006;Tamura et al.,2005). However, the performance degradation of ASHP at low ambient temperature has been a main issue for practical operation. Figure 3.2 illustrates the gap between heat output and a cabin heat load at the normal R134a refrigerant heat pump with respect to to the change of the outdoor temperature. In any heat pump, heating capacity decreases as the outdoor air temperature decreases. In contrast, the cabin heat load needed for the comfort cabin

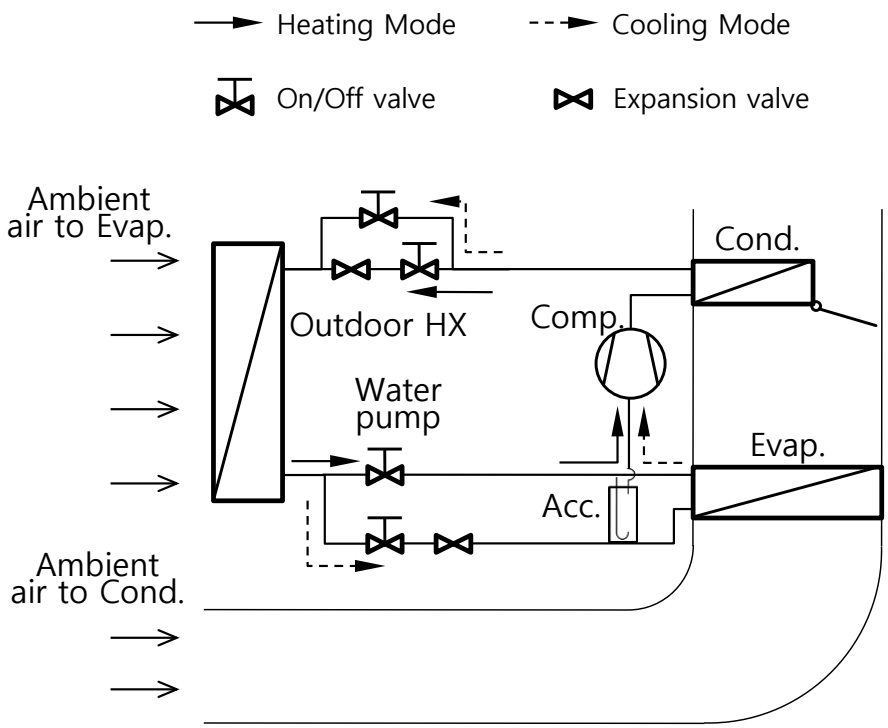

Figure 3.1 Schematics of basic air-source heat pump system for electric vehicle

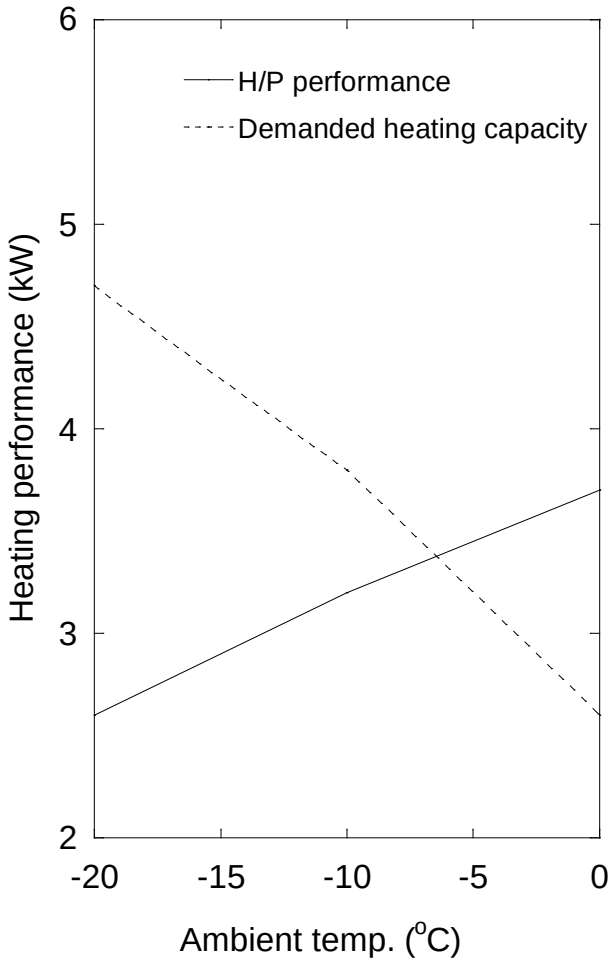

Figure 3.2 heating capacity vs heating demanding according to ambient temperature decrease (*Kwon*, TMSS 2014)

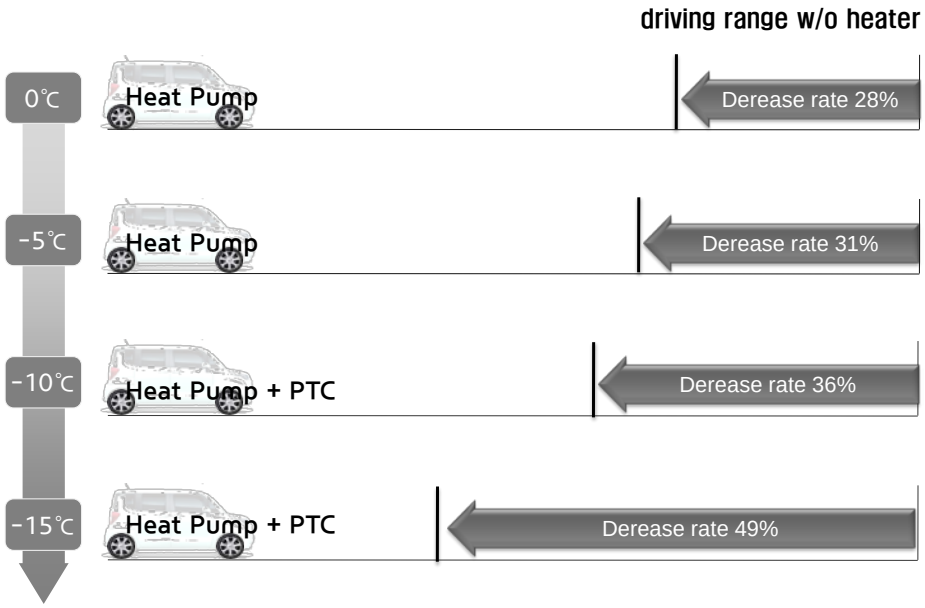

Figure 3.3 EV driving mileage change according to ambient temperature decrease (*Kwon*, TMSS 2014)

increases as the outdoor temperature drops. The deviation between the heat pump output and heat load should be supplemented by the PTC heater which consumes more electricity. As a result, it drastically reduces the EV driving mileage (Figure 3.3). For this reason, the performance of the EV heat pump system at a cold weather condition must be improved.

In this chapter, various heat pump systems are proposed to improve the heat pump performance in cold climate, and are experimentally evaluated for EV application. We call it cold climate heat pump (CCHP)

3.2 Heat pump system for EV

3.2.1 CCHP 1 : Heat pump with PE waste heat recovery

For EV application, we use a simple economical air-source heat pump because it only needs a few additional parts, like an indoor condenser and refrigerant valves. However, the performance of the air-source heat pump system degrades at low ambient temperature due to the reduction of refrigerant mass flow rate (Figure 3.4). As a result, the operation of the air-source heat pump system is restricted to a mildly cold condition.

EV has power electronics (PE) like motors, inverters and converters and PE results in heat loss. Although the heat source of PE waste heat does not have so high temperature for heating cabin directly, it can be a useful additional heat source for heat pump with deficient air heat source. In the previous study, an air source heat pump with EV PE waste heat recovery is proposed and is considered as a baseline CCHP. Note that in the heat pump with PE waste heat

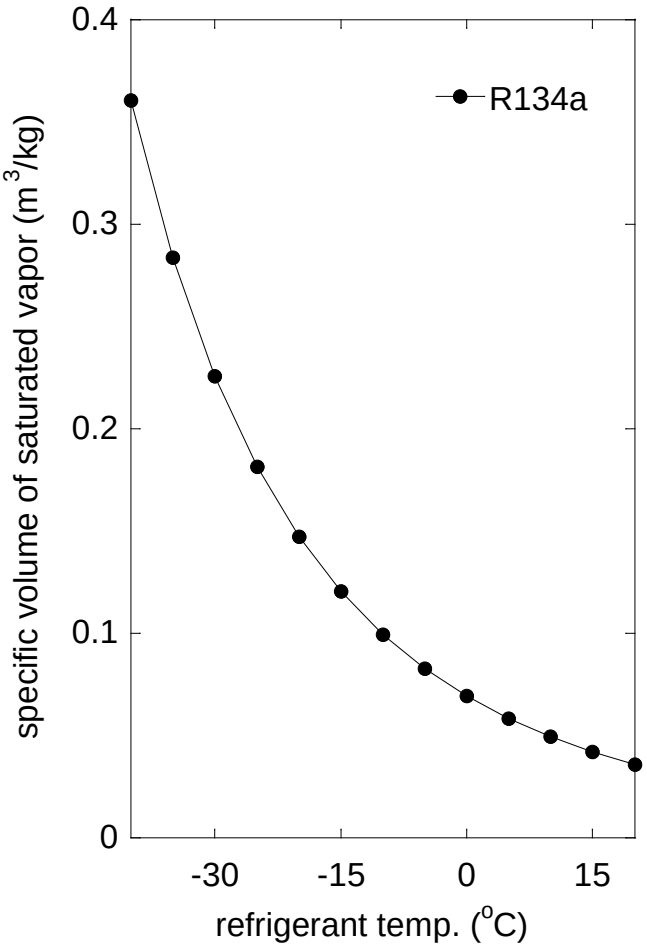

Figure 3.4 Refrigerant R134a specific volume of saturated vapor according to refrigerant temperature

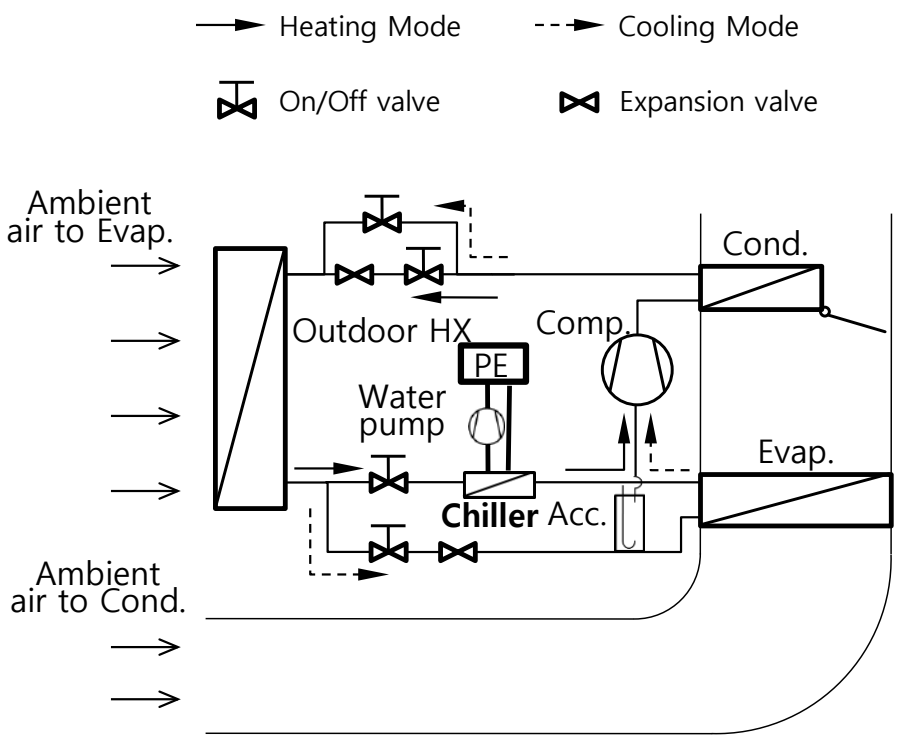

Figure 3.5 Description of CCHP1 : Heat pump with PE waste heat recovery

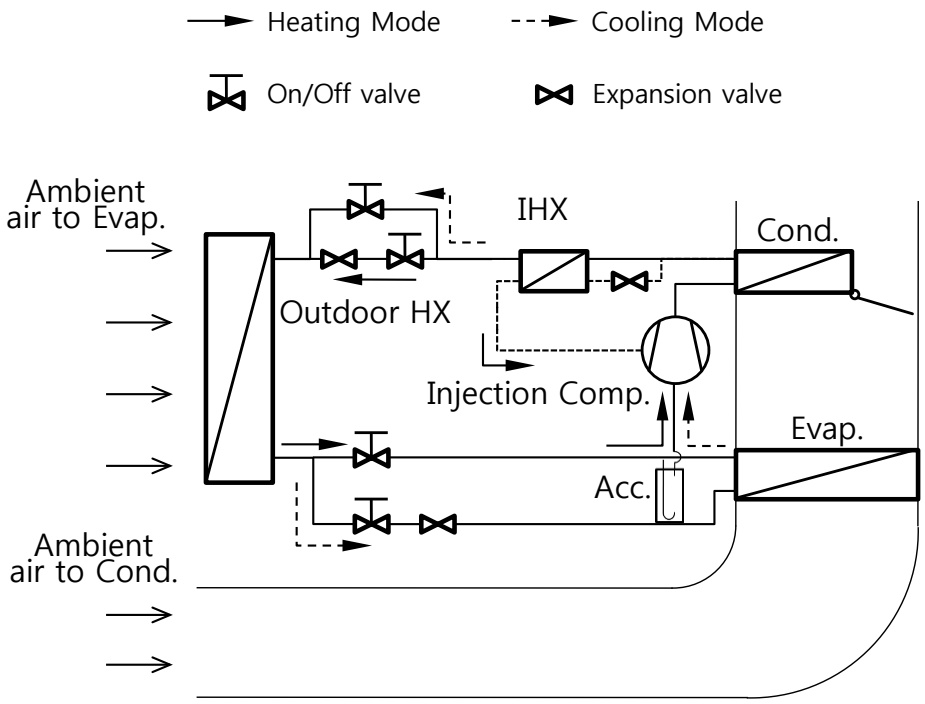

Figure 3.6 Description of CCHP2 : Vapor injection heat pump with one scroll electric compressor

recovery, an additional coolant circuit between PE and refrigerant heat pump cycle is added. In fact, the coolant system can be shared with PE cooling system, and only the heat exchanger (Chiller) should be located in the end of the outdoor evaporator, which absorbs the heat from coolant to refrigerant. In a bench test, PTC heat source replaces the real EV PE heat source (Figure 3.5).

3.2.2 CCHP2 : Vapor injection heat pump with 1 scroll comp

Vapor refrigerant injection for compressors has been actively studied in recent years (Heo et al.,2010;Aikins et al.,2013;Roh et al.,2014;Xing et al.,2011). Bertsch (2005) and Bertsch and Groll (2008) studied two-stage compression with vapor injection, which used compressors in series, i.e. a low stage compressor and a high stage compressor. This concept is difficult to be used to EV application, because of its high cost. Therefore we consider a vapor injection heat pump with 1 scroll compressor as shown in Figure 3.6. We use an internal heat exchanger (ihx) vapor injection of heat pump system because of the delicate refrigerant flow control method. The ihx vapor injection system needs additional parts, consisting of an additional heat exchanger and an electric expansion valve to control the flow of refrigerant, and an injection compressor. These additional components can be incorporated with the conventional EV heat pump system in an outdoor space, usually called the engine room.

3.2.3 CCHP3 : Heat pump with dual-parallel scroll single motor compressor (DPSC)

To improve heating capacity at low ambient temperatures, another solution is to use multi-capacity compressors like two compressors in parallel. The concept of two compressors is not appropriate for EV application due to limited space and cost. Therefore, we propose a dual-parallel scroll one motor compressor (DPSC). Figure3.7 shows the configuration of DPSC. DPSC has the same motor like the current compressor, but it can increase the maximum suction volume by two fold only, for the cold climate heat pump operation. Therefore, it has the same as the current single scroll compressor in other operational condition like cabin cooling.

The scroll and motor for EV compressor is usually designed for the maximum cabin cooling target. For cabin cooling, scroll torque is proportional to the cabin heat loss. However, for the cabin heating, the scroll torque is decreasing when the cabin heat load increases and motor torque is available. Although it can control various speeds, it cannot cover the required cabin heat load with the compressor scroll in cold climate condition. As it operates at the maximum speed in cold climate mode, the refrigerant mass flow rate decreases due to low density of refrigerant, and compressor consumes less torque and power. In other words, electric motor capacity is more than the load of refrigerant compression required in cold climate mode (Figure 3.8). If DPSC is only operated in CCHP mode, it can compress more refrigerant and increases the refrigerant mass flow rate with the same electric motor capacity. The 3rd CCHP is a heat pump with DPSC, which share the other heat pump

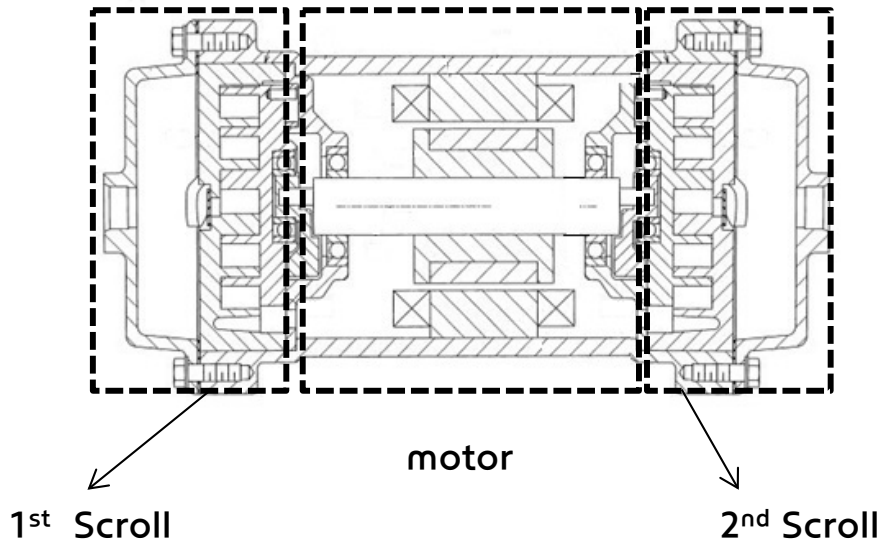

(a)

Figure 3.7 Description of
(a) DPSC, and
(b) CCHP3 : heat pump with dual-parallel scroll single motor compressor (DPSC) (Continued)

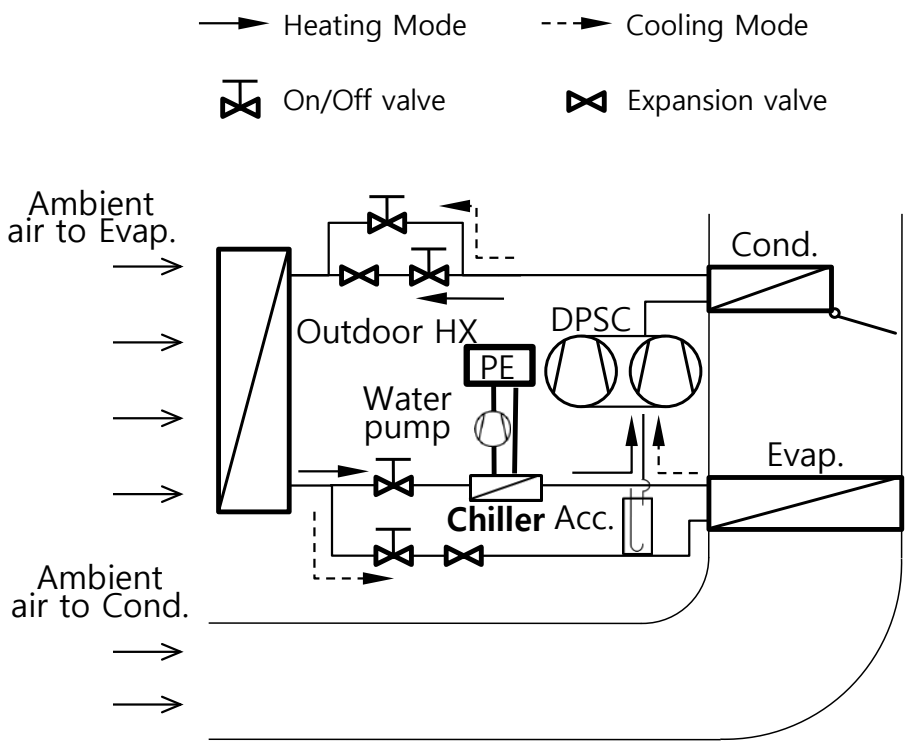

(b)

Figure 3.7 Description of

(a) DPSC, and

(b) CCHP3 : heat pump with dual-parellel scroll single motor compressor (DPSC)

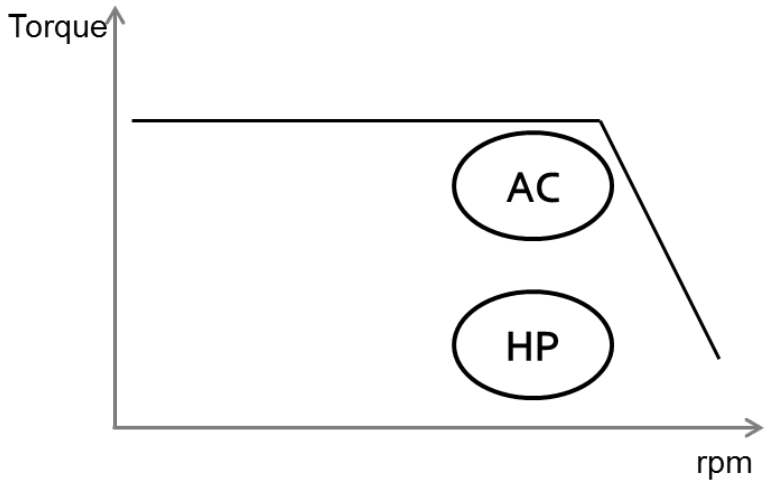

Figure 3.8 Operational torque characteristics for electric scroll compressor of electric vehicle (EV)

components with the baseline heat pump except for the compressor.

3.3 Experimental setup

3.3.1 Experimental scheme

Figure 3.9 shows the experimental schematic diagram of CCHP and experimental setup. The test facility consists of two climate control chambers, which can control the air temperature and humidity. This test facility can be available for an HVAC system calorimeter according to the SAE J2765.

This test facility simulates both cabin side and engine room side. In cabin side, there is a HVAC module, which consists of an air intake, an indoor blower, and an indoor condenser. The other components for CCHPs, like an accumulator, an expansion valve, an outdoor evaporator, and an electric driven scroll compressor, are located in engine room side. In each chamber, there is air flow rate control duct channel. In cabin side, it is push-type, which pushes the chamber air to intake of HVAC. Engine room side has pull-type duct channel, which pull the chamber air to outdoor evaporator.

3.3.2 Description of CCHPs' configuration for experiments

CCHP1 has PE waste heat recovery system with the basic heat pump cycle, which is composed of a coolant circuit and a plate heat exchanger (chiller). The PE waste heat source is replaced by PTC water heater with 500W electric output. It is estimated by 10% of normal driving power at low speed.

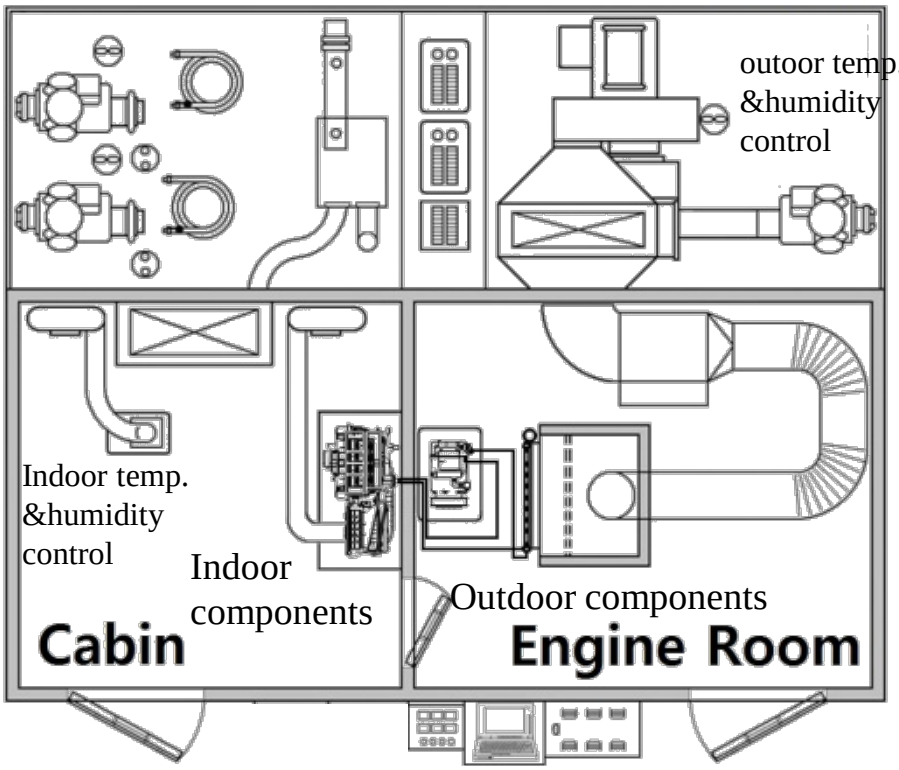

Figure 3.9 Schematic diagram of experimental facility

The coolant is mixture of 50% Ethylene glycol and 50% water. It is baseline for this study.

CCHP2 adds a vapor injection system to CCHP1. A vapor injection system consists of an injection expansion valve, ihx and a vapor injection hole in compressor scroll. For injection expansion valve, we use the metering valve, of which we can control the expansion rate by clock move. An internal heat exchanger is a plate heat exchanger. Injection hole is located at 240° at which refrigerant mass flow rate can be maximally increased.

CCHP3 is a heat pump with DPSC. This study is to investigate the heat pump performance with DPSC. We replace DPSC with parallel connected two scroll compressors that operate at the same speed, because of the limit of time and cost. The other components are as same as CCHP1.

3.3.3 Data reduction

We collected experimental data from both the air side and the refrigerant side. At the inlet and outlet of the each heat exchanger, the compressor, and outlet of the expansion valve, K-type thermocouples and pressure transducers were used to measure the temperature and pressure. Mass flow rate of the refrigerant was measured by Coriolis type mass flow meter by Oval (Ultra Mass MK-2). We analyzed and compared the two data sets obtained from the air side and the refrigerant side., The deviation was within 5%. As the data of air side was more stable than that of refrigerant side, we used the air-side data as reference. To determine the heating capacity of the two data sets, we used the enthalpy method and equations are given by :

$$\dot{Q}_{heat} = \dot{m}_{air} C_p \Delta T_{air,evap} \tag{1}$$

$$\dot{Q}_{heat} = \dot{m}_{ref} \Delta h_{evap} \tag{2}$$

$$COP = \frac{\dot{Q}_{heat}}{\dot{W}_{comp}} \tag{3}$$

The test conditions were determined to invest each CCHP's characteristic performance. In table 00, we designed the test condition at various operating condition of the baseline heat pump (CCHP1) to characterize heat pump performance. Operating conditions are as follows:

- Compressor rpm variation
- Intake air flow rate variation
- Intake air mixture between cabin and outdoor air
- Outdoor evaporator air flow rate variation
- PE waste heat source variation
- Refrigerant charge rate variation
- Ambient temperature variation

In CCHP2, we tested the performance variation according to main expansion valve as well as the injection valve opening rate.

In the case CCHP3 test, the first one is purposed to compare the CCHP mode performance. And the second one is to study the CCHP3 in mild climate condition.

3.4 Analysis of the experimental results

Various CCHPs proposed in previous section were tested in CCHP mode (ambient temperature-20℃). In CCHP mode, heating capacity is one of the most important performances for cost-effective EV heat pump application. Moreover COP also should be considered seriously because of the driving mileage extension. In this section, the test results are analyzed considering the EV application.

3.4.1 Performance analysis of the baseline CCHP1

As shown in section 2.1, heat pump with PE waste heat recovery is CCHP1. With CCHP1, we would like to investigate the heat pump characteristics in cold condition according to various operational conditions. We set up the various cases in Table 3.1. It can cover the effect on heat pump performance in cold climate by each component operational limit, which includes the compressor rpm, flow rate and temperature of condenser, air flow rate of outside evaporator, and PE waste heat.

Figure 3.10a is heat capacity and COP of heat pump at various operational

Table 3.1. Test conditions for CCHP1

Case no.	Amb. temp. (℃)	Air flow to cond. (m^3h^{-1})	Mixed air temp.to cond. (m^3h^{-1})	Mixed air to evap. (m^3h^{-1})	Comp. rpm (rpm)	PE waste heat (W)
1 (Baseline)	-20	300	-20	1950	5000	500
2	-20	300	-20	1950	7000	500
3	-20	450	-20	1950	5000	500
4	-20	300	-10	1950	5000	500
5	-20	300	-20	3120	5000	500
6	-20	300	-20	1950	5000	0

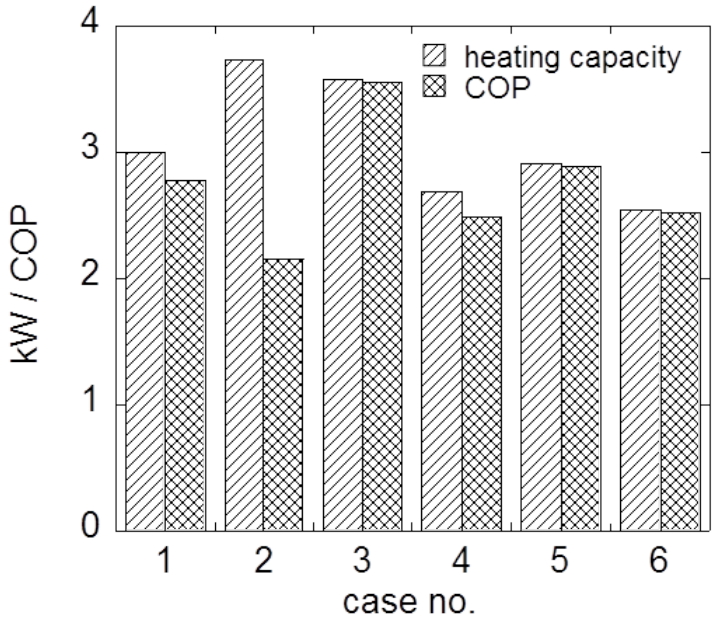

(a)

Figure 3.10 Experimental result of CCHP1 according to various operational variations,
(a) heating capacity and COP
(b) oulet discharge air temperature (ODAT)
(c) refrigerant mass flow rate (Continued)

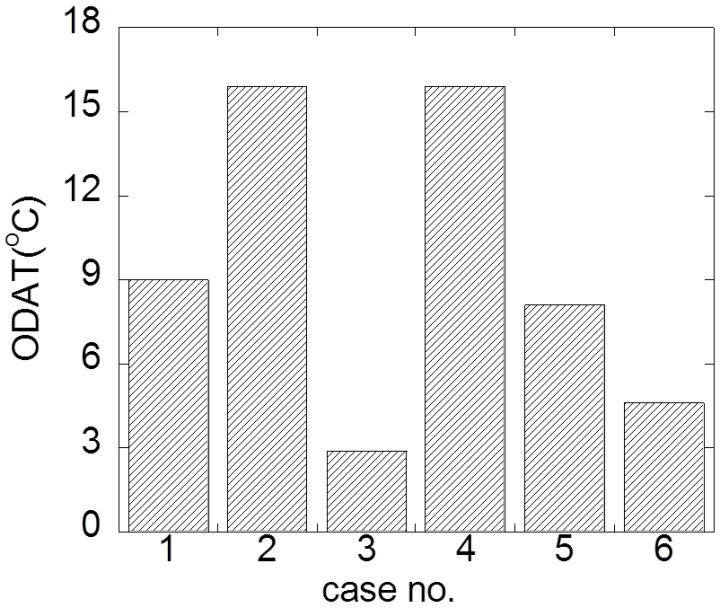

(b)

Figure 3.10 Experimental result of CCHP1 according to various operational variations,
(a) heating capacity and COP
(b) oulet discharge air temperature (ODAT)
(c) refrigerant mass flow rate (Continued)

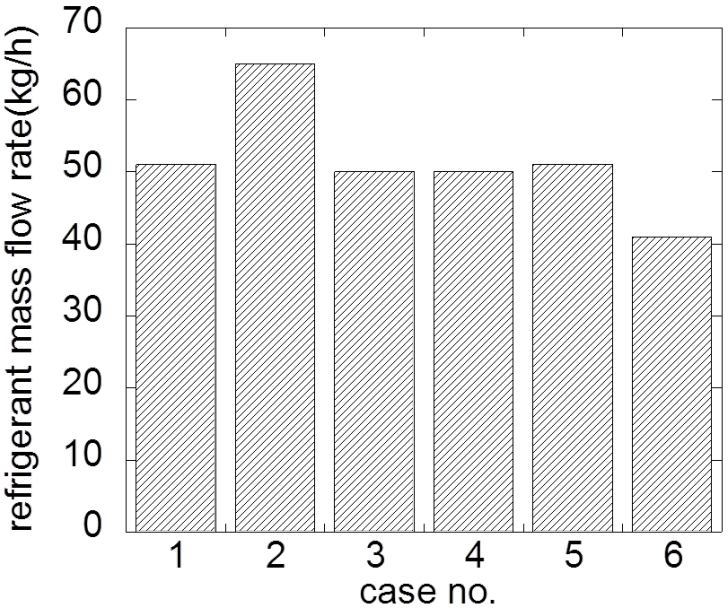

(c)

Figure 3.10 Experimental result of CCHP1 according to various operational variations,
(a) heating capacity and COP
(b) oulet discharge air temperature (ODAT)
(c) refrigerant mass flow rate

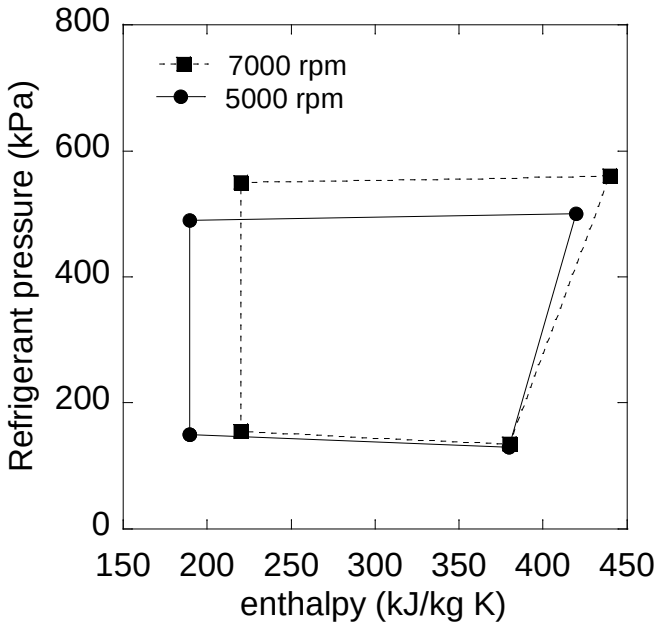

Figure 3.11 P-h diagram of CCHP according to compressor rpm increase

cases, and Figure 3.10b is the outlet air temperature (ODAT) of condenser. Mass flow rate of refrigerant can be seen in Figure 3.10c. We compared each case with the baseline case for CCHP1 .

At first, as we increased the compressor rpm limit from 5,000 to 7,000 rpm by 40 %, the mass flow rate of the refrigerant increased by 27 % and heating performance also increased by 24 %. Of course, OAT increased by 6.9℃. However COP decreased by 22 %. The compressor operation simultaneously increases the heating capacity and refrigerant mass flow rate, but it also raised the pressure of refrigerant as shown in Figure 3.11.

As we increased the air flow rate of the condenser by 50 % considering bigger powered blower, both the heating capacity and COP were improved by 19 % and 28 %, respectively. Because additional air flow of the condenser increased the subcooled temperature of the refrigerant and decreased the refrigerant high pressure.(Figure3.11) However ODAT decreased ODAT by 6.1℃ because of lower high pressure, and conditioned air further goes out. This increased the ventilation loss and total heat load more than heating capacity gain.

When we mix outside air and cabin air with the inlet air of condenser, air temperature of condenser can be increased. Case 4 was for approximately 20 % of cabin air volume flow rate mixed with 80 % of outside air volume flow rate. As air temperature into condenser was higher by 10℃ than the baseline (case1), both the heating capacity and COP were decreased by 10 %. Because the temperature difference between air and refrigerant in condenser shrinks, subcooled temperature decreases and high pressure increases. However

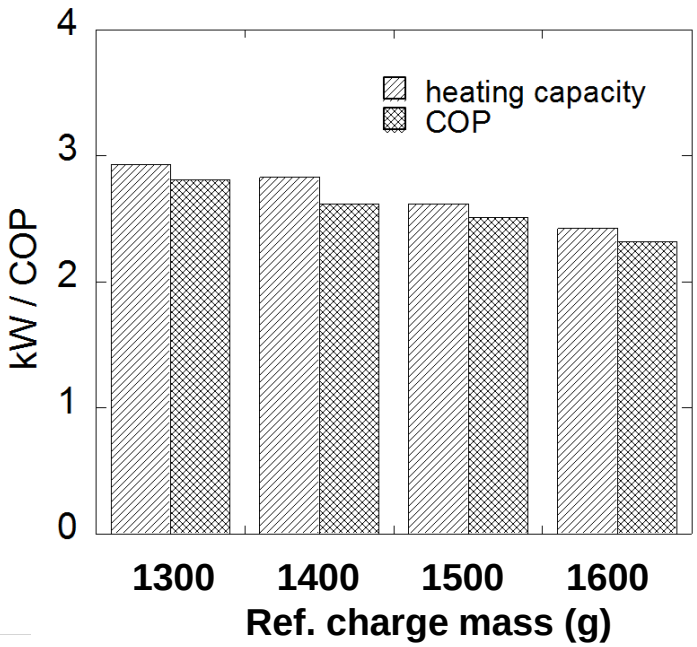

Figure 3.12 heating capacity and COP according to refrigerant charge rate in VI heat pump system

ODAT increased by 6.9℃ and the increase of recirculated air can reduce the ventilation loss more than heating capacity loss rate.

As we increased the air flow rate of evaporator by 60 %, COP increased little by 4 % and heating capacity decreased a little by 3 %. It was almost the same as the baseline because the outside evaporator was big enough to absorb the outside heat.

For PE waste heat recovery, we compared performance difference between non-heat source and 500W heat source. When we removed the PE heat source, the heating capacity and COP simultaneously decreased as we expected. The decrease of heating capacity was similar to that of PE heat source, and refrigerant mass flow rate decreased by 20%. From these results, PE waste heat recovery is imperative to increase heat capacity and COP in cold climate.

At last, we tested the change of the refrigerant charge rate. When we charged more by 23 %, both the heating capacity and COP decreased linearly with the increase of pressure ratio and the decrease of refrigerant mass flow rate (Figure 3.12).

3.4.2 Performance analysis of the CCHP2 and CCHP3

As shown in section 2.2, vapor injection heat pump with 1 scroll compressor is CCHP2. There are numerous previous studies for vapor injection heat pump. Among them, Kwon et. al. (2014) analytically evaluated EV application and it assumes that the superheat should be controlled well in the suction scroll and injection site. In this study, we would like to investigate

the CCHP2 performance with three kinds of commercialized main expansion valves (Table 3.2) and metering valve turns. (Figure 3.13)

Without injection, main expansion valves did not affect the heating capacities. As injection metering valve was turned more, heating capacities tended to be increased. The maximum heating capacity happened in 4 injection metering valve turn with the smallest expansion valve (EXV1), which was greater by 11% compared to the non-injection baseline. However COP trend was different. COP did not change or decreased. Within 0.5 turn of the metering valve, superheat of injection refrigerant might finish. And COP decreased by 17% at the maximum heating capacity. As we turned injection metering valve more, mass flow rates of the refrigerant increased by approximately 50% and OAT also increased by maximum 3.2℃.

As shown in section 3.2.3, CCHP3 is heat pump with DPSC. In the test of CCHP3 in cold climate condition, heating capacity drastically improved by 42% with 25% increase of refrigerant mass flow rate. However COP also decreased by 31% because of the increase of compressor work and pressure ratio. (Figure 3.12)

In Figure 3.14, we compared all the CCHPs prescribed. Compared to CCHP1 (baseline), CCHP2 was able to improve the heating performance by 8 % while we maintained the same level of COP with CCHP1. CCHP2 could improve the heating performance by 42 % and increase the OAT by 12℃ while COP level drops by 31 %. The increase of refrigerant mass flow rate was almost the same with that of CCHP2 and CCHP3. They were higher by ~ 25% than baseline CCHP1.

Table 3.2 Component specs. for CCHPs

Component	Type	Specification
Compressor	Electric scroll compressor (injection hole @ 240˚)	High voltage, 5kW capacity (33cc/rev)
Outdoor evaporator	Air to refrigerant compact heat exchanger	W570×H380×D20 (mm)
Indoor condenser	Air to refrigerant compact heat exchanger	W181×H175×D20 (mm)
Indoor evaporator	Air to refrigerant compact heat exchanger	W274×H228×D45 (mm)
Chiller	Water to refrigerant plate heat exchanger	W140×H70×D49 (mm)
IHX	Refrigerant to refrigerant plate heat exchanger	W90×H53×D23 (mm)
Main expansion valve	Orifice	Φ1.0/2.0/3.0 (mm)
Injection expansion valve	Variable orifice	Swagelok metering valve (SS-4MG-MH)

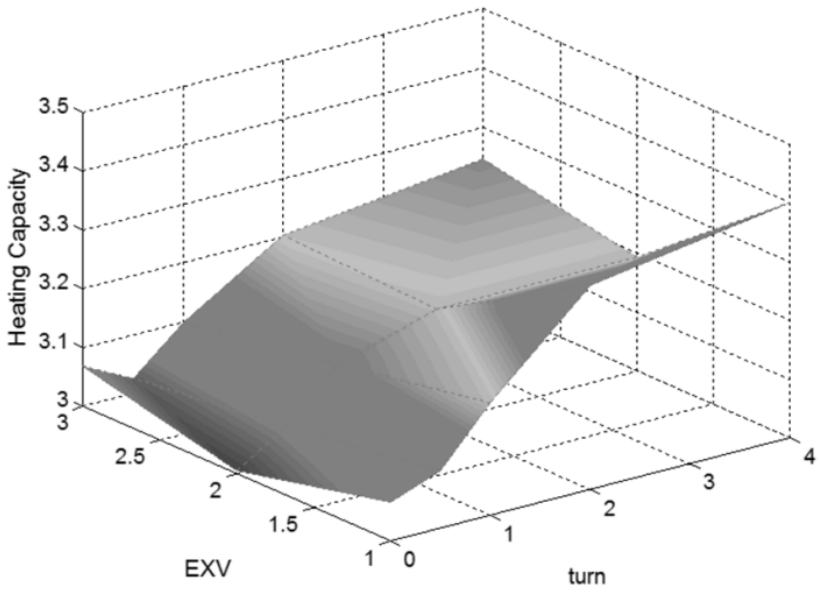

(a)

Figure 3.13 Experimental result of CCHP2 according to main expansion valves and injection valves' change
(a) Heating capacity,
(b) COP,
(c) oulet discharge air temperature (ODAT),
(d) refrigerant mass flow rate (Continued)

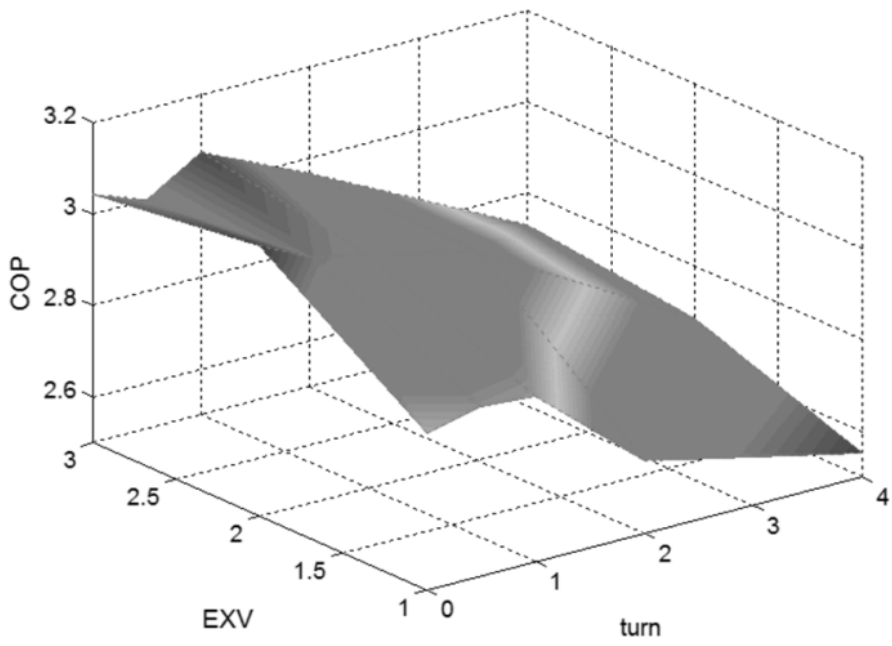

(b)

Figure 3.13 Experimental result of CCHP2 according to main expansion valves and injection valves' change
(a) Heating capacity,
(b) COP,
(c) oulet discharge air temperature (ODAT),
(d) refrigerant mass flow rate (Continued)

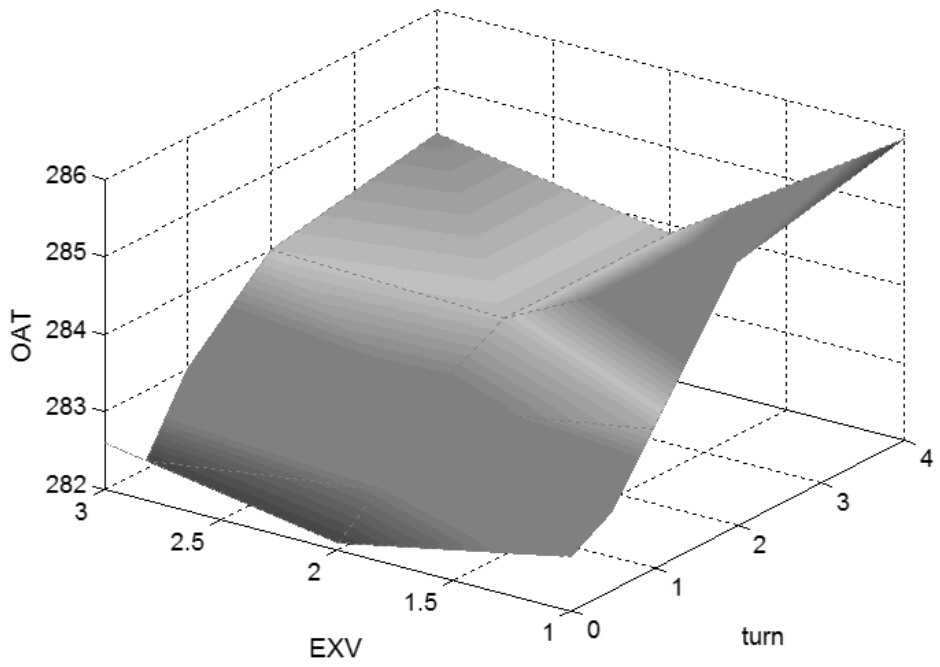

(c)

Figure 3.13 Experimental result of CCHP2 according to main expansion valves and injection valves' change
(a) Heating capacity,
(b) COP,
(c) oulet discharge air temperature (ODAT),
(d) refrigerant mass flow rate (Continued)

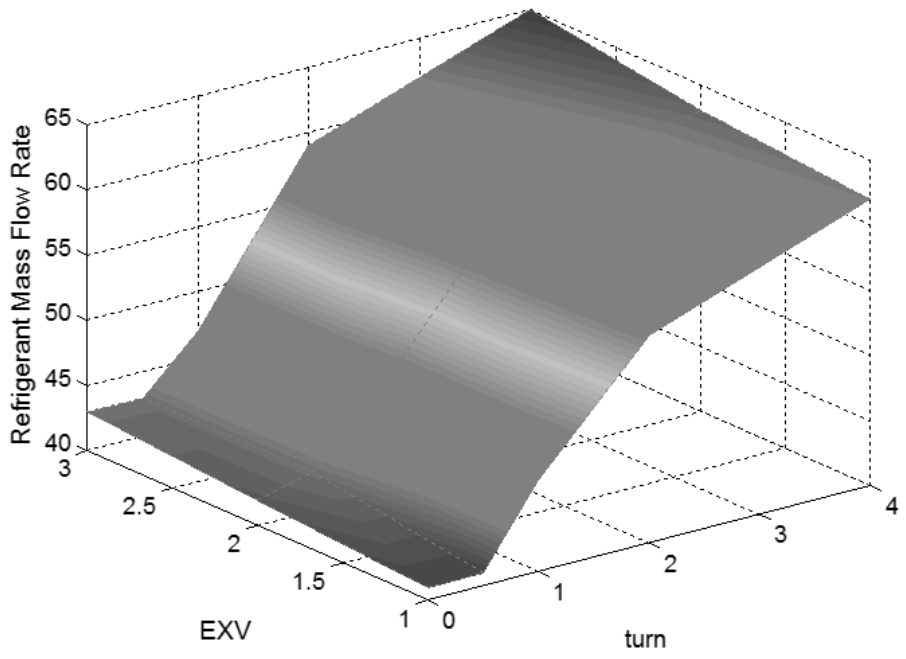

(d)

Figure 3.13 Experimental result of CCHP2 according to main expansion valves and injection valves' change
(a) Heating capacity,
(b) COP,
(c) oulet discharge air temperature (ODAT),
(d) refrigerant mass flow rate

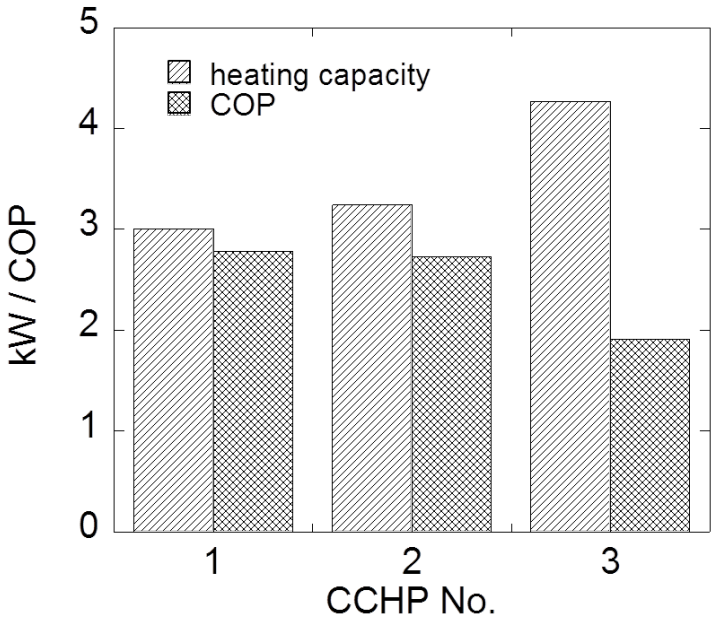

(a)

Figure 3.14 Comparison between CCHPs about
(a) heating capacity and COP,
(b) oulet discharge air temperature (ODAT),
(c) refrigerant mass flow rate (Continued)

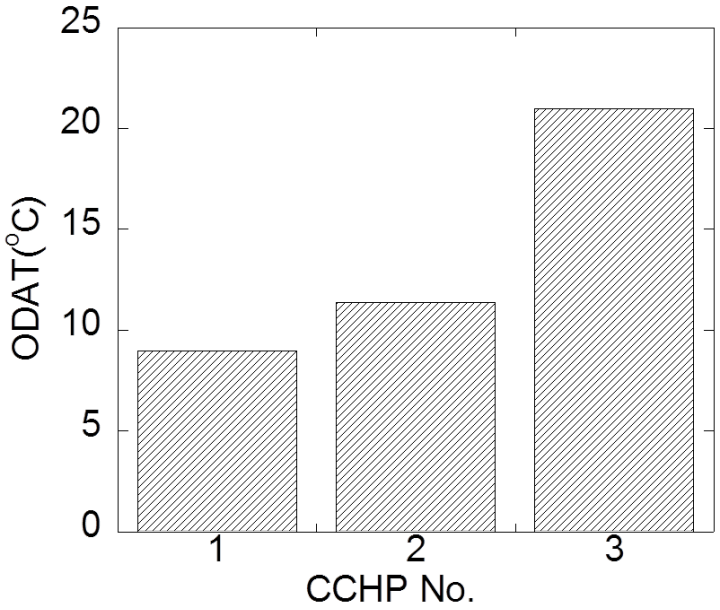

(b)

Figure 3.14 Comparison between CCHPs about
(a) heating capacity and COP,
(b) oulet discharge air temperature (ODAT),
(c) refrigerant mass flow rate (Continued)

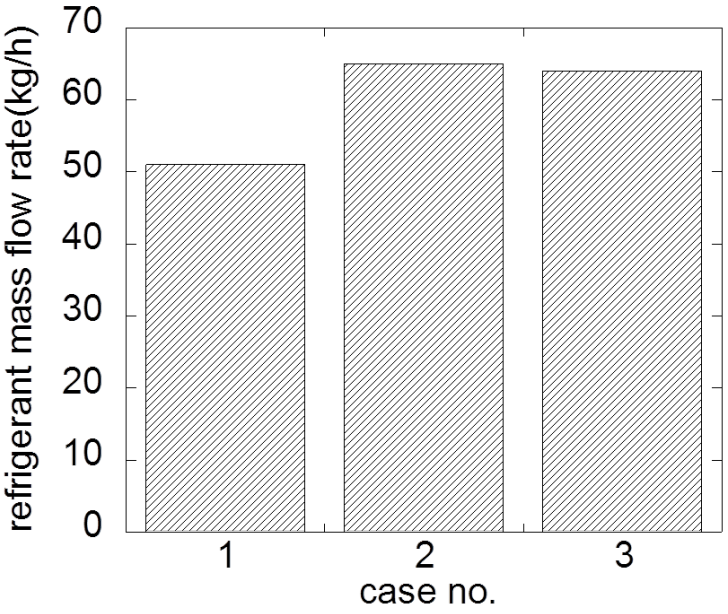

(c)

Figure 3.14 Comparison between CCHPs about
(a) heating capacity and COP,
(b) oulet discharge air temperature (ODAT),
(c) refrigerant mass flow rate

3.4.3 Discussion

As we have discussed in previous sections, current heat pump for EV had an insufficient heating capacity in cold climate condition. Therefore three CCHPs were proposed and the improvement of the heating capacity was validated. Heating capacities of CCHP1, CCHP2, and CCHP3 were improved by 10%, 8%, and 42%, respectively. If they were combined, the improvement of total heating capacity would be 68%. If we used CCHP1 as baseline, total CCHP could improve heating capacity by 54 %.

At last, we would like to validate the heating capacity of all CCHPs, so we did the validation test for total CCHP. Heating capacity of total CCHP was improved by 61% compared to CCHP1 alone. Total CCHP, however, is not sufficient for cabin heat load, but the gap between heating capacity and cabin heat load was greatly decreased. Its ODAT were 28℃ and this needs small improvement in cold condition. If we use the operational variation like recirculated air mix or compressor rpm increase, it could cover the gap.

2.5 Conclusions

For the extension of EV driving range, efficient heat pump application is imperative. If we need to use EV heat pump, we should develop the cost-effective, high performance heat pump in cold climate (CCHP). In this paper, we proposed the three kinds of CCHPs and experimentally investigated their performance, configuring them with automotive heat pump components. And we could figure out that they could be the solutions. We can summary this

study as below:

1. To reduce the gap between heating capacity and cabin heat load, we need to increase compressor rpm, recirculated air mix, PE waste heat recovery, vapor injection, and DPSC.
2. Among the parameters in 1, only both the PE waste heat recovery and vapor injection had similar or improved COP.
3. CCHP3 with DPSC and the increase of compressor rpm significantly influences the heating capacity in cold weather.
4. The increase of total CCHP with compressor rpm and recirculated air mix could meet the cabin heat load in cold weather.

In conclusion, total CCHP could be a cost-effective, high performance CCHP for EV application. In the future work, it is necessary to incorporate total CCHP to real EV and validate it in vehicle level.

Chapter 4. Validation of heating performance with advanced cold climate heat pump in a test vehicle

4.1 Introduction

The efficient and economic heating system determines the driving range and cost of EVs, two of the most important remaining issues to make EVs prevail on the road over gas-powered vehicles. A heat pump could be the best solution to extend the driving range in mild-winter climates, but its performance quickly degrades as the temperature goes down. Therefore, a high-voltage positive temperature coefficient (PTC) heater is usually added to the heating system when a heat pump is used, which requires high voltage and is expensive. To overcome these limitations of a high-voltage PTC heater and improve the heating performance of an EV in cold weather, an alternative, economical heating system is highly desirable.

In the previous chapters, we proposed three new types of heat pump, called cold climate heat pump (CCHP), and investigated their experimental performance on a test bench together with automotive HVAC components. The experiments confirmed that CCHPs improved the heating performance by 8%~40% in the cold climate condition. This performance improvement is impressive, but we are not yet confident whether we can use the CCHP without a high-voltage PTC heater. It is because the cabin thermal load, which

can affect the real heating performance and the real driving range of a vehicle, cannot be accurately estimated by the test bench experiments or system-level test.

The heating load of a vehicle typically includes transient heating of thermal mass(cabin interiors), convectional loss and ventilation loss (Kowsky et al.,2012). The transient heating depends on thermal mass inside the cabin, interior geometry of the cabin and its heat transfer characteristics. The convection term depends on vehicle speed, wind speed, the direction of wind over the vehicle, etc. The ventilation loss depends on the infiltration of air into the cabin and intended ventilation fresh air. There is a recent work on modeling cabin thermal load (H.Youmans, 2011, ASHRAE data), but the method is too complex and the accuracy in real-world conditions is questionable. Furthermore, there are important parameters for HVAC control that cannot be predicted at a system level. For example, some air is recirculated into the cabin to reduce the thermal load, but the exact amount of recirculation cannot be determined at a HVAC system level. Therefore, a real-world vehicle-level tests were essential to accurately evaluate the heating performance and power consumption, and thus to fairly determine the feasibility of the proposed CCHPs.

In this chapter, we described a vehicle-level test for the proposed CCHPs and checked the feasibility of operating the CCHP without a high-voltage, high-capacity PTC heater or with a low-voltage, low-cost PTC heater by comparing the cabin heating performance and electric power consumption..

4.2 Test vehicle preparation

4.2.1 Description of test vehicle

The test vehicle used in this study was Kia Soul EV, a compact crossover sport utility vehicle (SUV) with a 27 kWh lithium-ion polymer battery (Figure 4.1). The vehicle was originally equipped with a heat pump system with PE waste heat recovery and a high voltage PTC heater (Table 4.1). After baseline testing, the original heat pump was replaced with the proposed CCHP as described in the next section.

4.2.2 Installation of advanced CCHP

In Chapter 3, we proposed three types of CCHPs:

- PE waste heat recovery
- Vapor injection
- Dual-Parallel scroll Single motor Compressor (DPSC)

The heat pump in Kia Soul EV was installed with a PE waste heat recovery unit consisting of an electric water pump and a plate-type heat exchanger. We used the original system for a baseline measurement before testing CCHP at the vehicle level. For testing CCHP, we used most of the original heat pump components without any changes but replaced a few components for the DPSC with a vapor injection system as listed in Table 4.2. The orifice size for vapor injection was chosen based on the system-level experiments.

The system-level experiments in cold weather conditions suggested that

Figure 4.1 Kia Soul EV for CCHP installation (*www.Kia.com*)

Table 4.1 Component specs for baseline heat pump of Soul EV

Component	Type	Specification
Compressor	Electric scroll compressor	High voltage, 5kW capacity (33cc/rev)
Outdoor evaporator	Air to refrigerant compact heat exchanger	W570×H380×D20 (mm)
Indoor condenser	Air to refrigerant compact heat exchanger	W181×H175×D20 (mm)
Indoor evaporator	Air to refrigerant compact heat exchanger	W274×H228×D45 (mm)
Chiller	Water to refrigerant plate heat exchanger	W140×H70×D49 (mm)
Electric auxiliary heater	PTC heater	W200×H186×D28 (mm) 6kW capacity

installing a DPSC was the most influencing factor for improving the heating performance. Therefore, we used DPSC for all the tests. The other experimental parameters included for the vehicle-level tests were vapor injection, compressor rpm and recirculated air mixture (Table 4.3). For seven different combinations of these parameters, we compared heating performance, consumed electric power and installation.

4.2.3 Test setup

Heating performance and consumed electric power of heat pumps are the most important parameters to be measured in the vehicle level tests. The heating performance at a vehicle level can be quantified as the average cabin temperature and the ODAT (outlet discharged air temperature) into the cabin. To measure these, we installed K-type thermocouples at the breath and foot positions in each seat and at the HVAC duct outlets. The positions of installed thermocouples are shown in Figure 4.2.

For calculating heating performance, we measured both the refrigerant and air temperatures. However, the mass flow rate of refrigerant were hard to measure due to the complex geometry of the cooling system. Therefore, we calculated the heating performance using the air temperatures:

$$\dot{Q}_{heat} = \dot{m}_{air} C_p \Delta T_{air,evap}$$

Two electric scroll compressors are needed for DPSC operation. For calculating the consumed electric power, we used an internal power control

Table 4.2 Component specs for advanced CCHP installed on Soul EV

Component	Type	Specification
Compressor (2EA)	Electric scroll compressor (injection hole @ 240˚)	High voltage, 5kW capacity (33cc/rev)
Outdoor evaporator	Air to refrigerant compact heat exchanger	W570×H380×D20 (mm)
Indoor condenser	Air to refrigerant compact heat exchanger	W181×H175×D20 (mm)
Indoor evaporator	Air to refrigerant compact heat exchanger	W274×H228×D45 (mm)
Chiller	Water to refrigerant plate heat exchanger	W140×H70×D49 (mm)
IHX (new)	Refrigerant to refrigerant plate heat exchanger	W90×H53×D49 (mm)
Main expansion valve (new)	Orifice	Φ1.0/2.0/3.0 (mm)
Injection expansion valve (new)	Variable orifice	Swagelok metering valve (SS-4MG-MH)

Table 4.3 Experimental parameters for vehicle-level tests

CCHP no	Case #1	Case #2	Case #3	Case #4	Case #5	Case #6	Case #7	Base-line
DPSC	O	O	O	O	O	O	O	X
Vapor injection	O	X	X	X	O	O	O	X
Comp rpm	5,000	5,000	6,000	5,000	5,000	5,000	7,000	5,000
Recirculated air mixture (60%)	X	X	O	O	O	O	O	X
Auxiliary PTC heater	X	1 kw low	1 kw low	1.4 kw low	X	1 kw low	X	6 kw high

* low : low voltage PTC heater

high : high voltage PTC heater

Figure 4.2 Positions for cabin temperature measurement

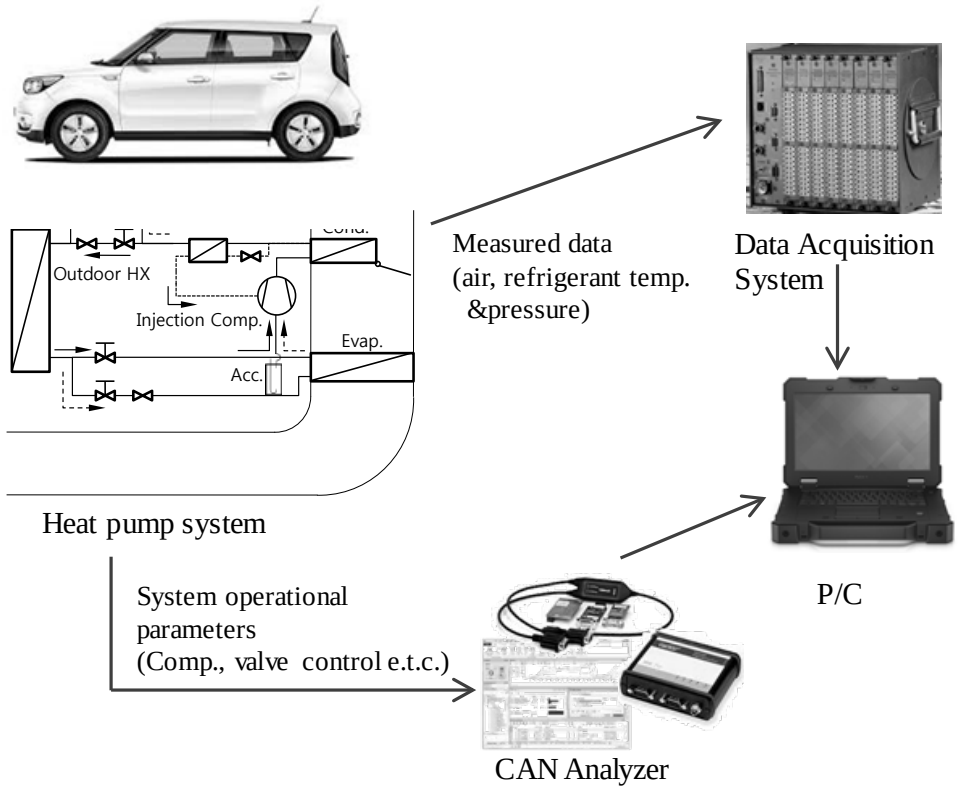

Figure 4.3 Data aquasition description for the vehicle test

module that is connected to each electric scroll compressor. The internal power control module monitors the current and voltage of each compressor and sends the information to the Controller Area Network (CAN) system of the vehicle. The coefficient of performance (COP) for the heat pump at vehicle level operation can be calculated from

$$COP = \frac{\dot{Q}_{heat}}{\dot{W}_{comp}}$$

Figure 4.3 shows the experimental setup for the vehicle-level tests. We followed the general procedure for vehicle heater test including overnight soaking and driving in the highest heating operation mode. (50kph for 20 minutes with maximum heater control set) We set the maximum HVAC blower flow rate at 300 CMH and operated the compressors for heat pump at 5000 rpm. The target heating performance was to reach 18 ºC in 20 minutes after heater operation at the ambient temperature of -20 ºC, which is done in the same vehicle powered by an internal combustion engine .

4.3 Vehicle test result in cold climate

We conducted vehicle-level tests in three steps. First, we compared the CCHP's heating performance with the target for different combinations of test parameters. Secondly, we calculated the electric power consumption if the heating performance meets the target. Lastly, we conducted an additional regulation test, windshield defrosting, which is mandatory.

4.3.1 Heating performance

The vehicle-level heating performance was calculated from the average temperature in the cabin. The target heating performance was to reach 18 ºC in 20 minutes after heater operation. The baseline system without a PTC heater reached only -4 ºC in 20 minutes; the cabin temperature needed to be further increased by 22 ºC. In Test #1, we operated both the DPSC and the vapor injection system. The final temperature was about 4 ºC. The system-level test showed that increasing the refrigerant mass flow rate increased the heating performance by 25% (3.4.2). Even if we assume that the same level of improvement in heating performance can be achieved at the vehicle level, it is not sufficient to reach the target. When we use vapor injection and air mixture recirculation (test #5), the heating performance was significantly improved and the final temperature reached about 14 ºC. However, it still did not meet the target. Using a 1 kW PTC heater in conjunction with vapor injection and air mixture recirculation (test #6), we could almost meet the target; the final temperature was about 19 ºC. The 1 kW PTC heater uses low voltage, and thus is less expensive and consumes less power compared to the 5 kW high-voltage PTC heater currently used with a heat pump. Therefore, the first candidate for an alternative heating system is the combination used in Test #6.

When we increased the compressor speed from 5,000 rpm to 7000 rpm instead of using a 1 kW PTC heater (test #7), we could also meet the target. However, when we increase the compressor speed, the compressor showed an unstable high-pressure dynamic feature: the pressure spiked and reached the

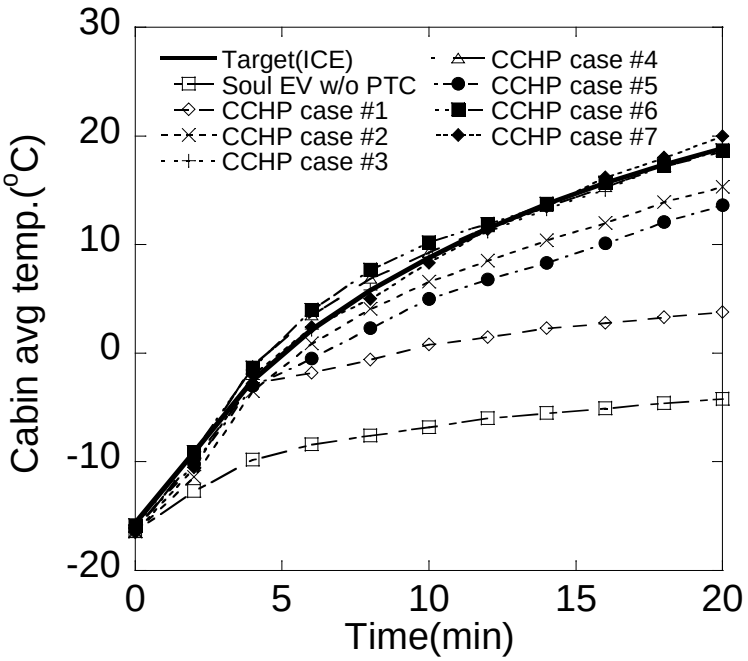

(a)

Figure 4.4 Heater performance results during warm up at -20℃

(a) Avg. cabin temperature,

(b) oulet discharge air temperature (ODAT)

(Continued)

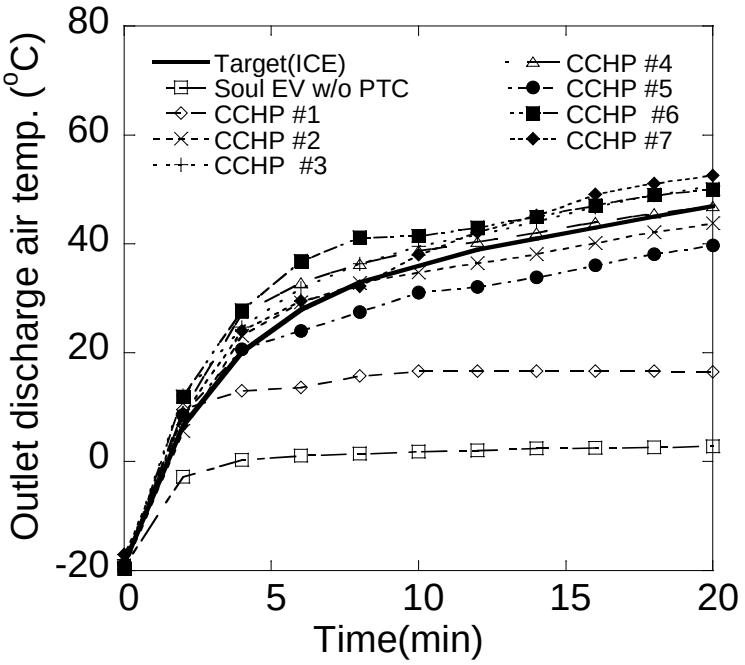

(b)

Figure 4.4 Heater performance results during warm up at -20℃

(a) Avg. cabin temperature,

(b) oulet discharge air temperature (ODAT)

Table 4.4 Heater performance summary according to experimental parameter changes (avg. cabin temp. and ODAT)

CCHP no	Case #1	Case #2	Case #3	Case #4	Case #5	Case #6	Case #7	Base-line (w/o PTC)
Cabin average temp. (℃)	3.8	15.3	19.0	18.6	13.6	18.7	20.0	-4.2
Outlet discharge air temp. (℃)	16.5	43.8	50.6	47.0	39.7	50.0	52.6	2.8
Target	Conventional engine vehicle heater performance							
Satisfaction	X	X	O	O	X	O	O	X

limit at the beginning of operation, which was not regulated by the expansion valve control.

The vapor injection technology needs significant modifications of the system and elaborated control. Therefore, we checked whether we could remove the vapor injection and still meet the target. In Test #2, when we operated the 1kW PTC heater together with recirculated air mixture, the final temperature was about 17ºC. Increasing the compressor speed from 5,000 rpm to 6000 rpm (test #3), the final temperature reached 19 ºC. Replacing the 1 kW PTC heater with a 1.4kW PTC heater (test #4), we could still meet the target.

In summary, we have identified 4 candidates (tests #3, #4, #6 and 7) for an alternative CCHP system that can provide as high heating performance as an equivalent IC engine vehicle.

4.3.2 Driving range prediction

In the previous section, we identified 4 candidates for an alternative CCHP system based on the heating performance. Electric power consumption is as important as the heating performance in determining a vehicle heating system, because it determines the driving range. We compared the power consumption by the compressor and PTC heater for the 4 test conditions selected in the previous section. We also measured the electric power consumption by the heat pump and 6 kW PTC heater that were originally installed in the Soul EV, and used it as a baseline for comparison. Note that the PTC heater was turned

on only when the target cabin temperature could not be met even after maximum heat pump operation.

Figure 4.5 shows the electric power consumption during heater warm up test for 4 CCHPs and the baseline. Table 5.5 summarizes total energy consumption, average electric power and the electric power at the steady state for the 4 test conditions and the baseline.

- case #4 < case #6 < baseline < case #3 < case #7 for transient state
- case #4 < case #6 < case #3 < baseline < case #7 for steady state

When the 0.4kW increase of PTC heater capacity compensated for the deficient heating performance of DPSC heat pump system, electric power consumption was saved by 11% for transient state (warm up), and by 29% for steady state compared to baseline. When the 1kW PTC heater was added for the vapor injection DPSC heat pump system, its power consumption was more than DPSC heat pump with 1.4kW PTC heater. Though, its electric power consumption was saved by 3% for transient state (warm up), and by 22% for steady state compared to baseline. However increasing the compressor operating rpm and refrigerant mass flow rate decreased the system operational efficiency. When compressor operational rpm was increased, both the DPSC heat pump with 1kW PTC heater and vapor injection DPSC heat pump without PTC heater, utilized more electric power than baseline in transient state. In fact, at first, CCHPs seemed to be low efficient because of high pressure ratio and low compressor efficiency during warm up. Therefore they

consumed more than baseline, and the discharge air temperature also was slightly higher than baseline.(figure 4.5, figure 4.4b) However at the end of heating test, which means the steady state, all cases except case #7 consumed similar or less electric power than baseline. In other words, CCHPs could be more efficient for a long drive.

After all, DPSC heat pump with 1.4kW PTC heater or Vapor injection DPSC heat pump with 1kW PTC heater could be a solution for efficient CCHPs.

4.3.3 Windshield glass defrosting test for regulation

For EV application, we should validate the defrosting performance in -18 ºC ambient temperature due to the regulation. So we conducted the defrosting performance for one of the CCHPs, DPSC heat pump with 1.4kW PTC heater. As shown in figure 4.6, it satisfies the regulation criteria.

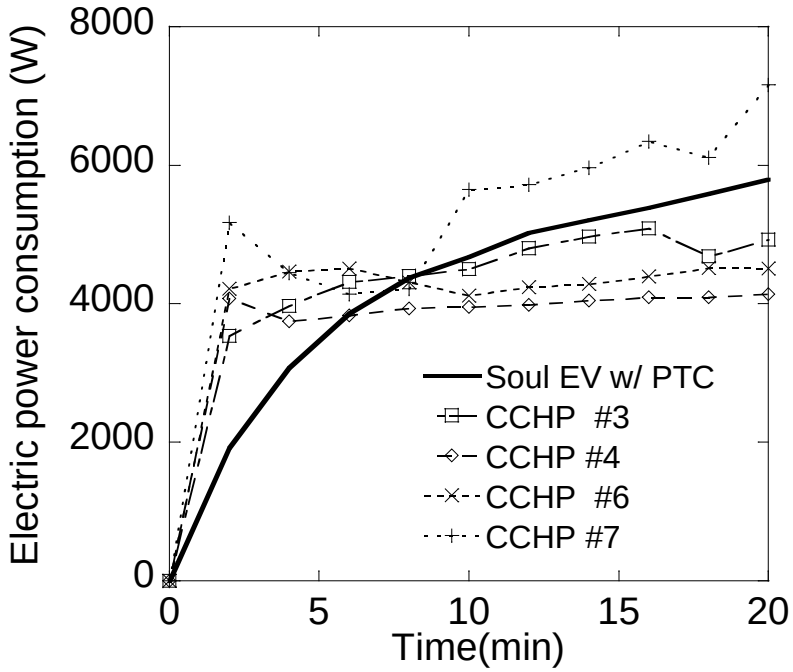

Figure 4.5 Electric power consumption result summary for the CCHPs satisfied for heater performance

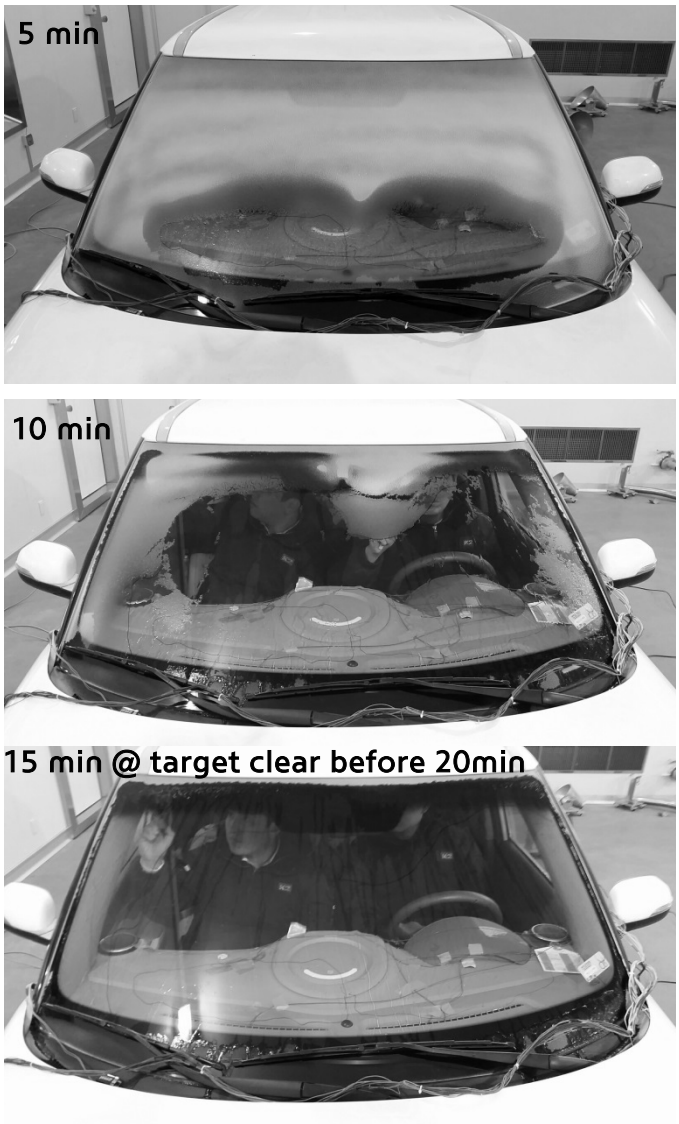

Figure 4.6 Windshield glass defrosting performance with CCHP for regulation

Table 4.5 Electric power consumption result summary for the CCHPs satisfied for heater performance

CCHP no	Case #3	Case #4	Case #6	Case #7	Baseline (w/ PTC)
Consumed electric energy (Wh)	1507	1330	1398	1831	1452
Average electric consumed power (W)	4520	3990	4193	5492	4355
Electric consumed power at steady state (W)	4924	4142	4508	7161	5393

4.5 Conclusions

We have tested the 7 cases of CCHP candidates in vehicle level, which was decided considering the system level experiences shown in chapter 3. Vehicle level testing was essential because the system level experiences could not consider the transient performance, in other words, the cabin thermal load change during soak and warm-up process. Therefore in this chapter, we have the vehicle level testing including the soak and warm-up process in the cold climate condition. To determine what case was more appropriate as an CCHP without high voltage PTC heater with high cost, heating performance, power consumption, and regulation performance by vehicle test were analyzed as follows :

1) EV CCHP without high voltage PTC heater is possible with refrigerant mass flow rate increase by DPSC or vapor injection and low voltage PTC heater
2) Recirculated cabin air mixture with fresh outdoor air should be included in the CCHP technologies
3) In cold climate condition, electric power consumption could be the least in DPSC heat pump with 1.4 kW low voltage PTC heater.
4) Vapor injection technology could be alternative for CCHP, but considering the required space and cost increase, DPSC heat pump with 1.4kW low voltage seems to be more efficient solution for CCHP.
5) Defrosting performance regulation also could be satisfied with DPSC

heat pump with 1.4kW low voltage.

In conclusion, this study shows that DPSC heat pump with 1.4 kW low voltage could be suggested as an good solution for CCHP considering performance and cost by vehicle level verification.

Chapter 5. Conclusions

Nowadays many car makers are developing and producing the battery electric vehicles (EVs) in the market, but they are facing lots of problems for enlarging EVs' market. Among them, two major tasks are the cost reduction and extending the driving range per a charge. This study was purposed to solve the problems by improving the cabin heating system of EV. As shown in the literature review of chapter 1, heat pump application is increasing for reducing the electric power consumption for cabin heating and enlarging the driving range in mild winter condition. Although heat pump was applied to EV and could save the electric power consumption in mild condition, it could not cover the cold climate condition because of the heat pump performance degradation according to ambient temperature down, but also EV still needed a high voltage additional positive temperature coefficient (PTC) heater, which leads an additional cost increase. In short, we investigated an advanced heat pump technologies to replace the high voltage additional PTC heater as we called it as a cold climate heat pump (CCHP).

To accomplish this goal, we considered the vapor injection technology first. It was well-known as a solution for cold climate heat pump in residential and industrial heat pump, but there were limited references for automotive industry. So in chapter 2, a baseline heat pump system was investigated and a vapor injection heat pump with internal heat exchanger (IHX) and injection compressor was designed for EV application. Analytical model for vapor

injection heat pump system was made through geometry-based thermodynamic approach for injection scroll compressor and the efficiency test database for other components. The simulation program were validated by comparing the predicted results with experimental data for non-injection condition in baseline heat pump system. By analyzing the experimental data for non-injection condition, we figured out the automotive heat pump characteristics as ambient temperature decreases. As the ambient temperature decreased, the heating capacity decreased, but COP increased because of the decrease of compressor work and the pressure ratio. We also analyzed the EV vapor injection heat pump system in cold condition. Application of the vapor injection technique to an EV heat pump increased the heating capacity and COP simultaneously in cold regions, and as outlet discharge air temperature (ODAT) was increased, the heating capacity for vapor injection system was increased while that for non-injection system was decreased. The COP for vapor injection system was better than that for non-injection system while COPs were decreased for all. Considering the COP characteristics of vapor injection system, it would be possible to utilize the optimum operation control with the same heating capacity and better COP. In chapter 2, we showed the characteristics of vapor injection heat pump in cold climate condition and suggested some insight of optimum control for reduced electric power consumption.

Although the vapor injection system could improve the heating capacity and COP, it was not possible to satisfy the proper cabin heating performance in cold climate condition. It was predicted by simulation in chapter 2. To

confirm the performance of vapor injection heat pump, an experimental approach was conducted in two ways of the system-level and vehicle level in chapter 3. As an CCHP concept, we proposed three kind of heat pumps. The first (CCHP1) was a heat pump with PE waste heat recovery. The second (CCHP2) was a vapor injection heat pump. The third (CCHP3) was a heat pump with Dual-Parallel scroll Single motor Compressor (DPSC), which is similar to tandem type heat pump, but use only one motor and dual scroll in cold climate. And we designed three kind of CCHPs and figured out the performance for them in system level experiments. Heating capacities of CCHP1, CCHP2, and CCHP3 were improved by 10%, 8%, and 42%, respectively. If they were combined, the improvement of total heating capacity would be 68%. If we used CCHP1 as baseline, total CCHP could improve heating capacity by 54 %. Among three CCHPs, CCHP1 and CCHP2 had similar or improved COP, but CCHP3 had the decreased COP. We also experienced the CCHPs' performance in various operating condition like the increase compressor rpm and recirculated air mix. Compressor rpm increase could improve the heating performance, but decreased the COP. Recirculated air mix decreased both of the heating capacity and COP, because of the pressure ratio increase. But it could increase the discharged air temperature. At the point of heating capacity in cold climate condition, it could be estimated that the increase of total CCHP with compressor rpm and recirculated air mix could meet the cabin heat load, but it needed vehicle level testing. Finally we validated the CCHPs in vehicle level in chapter4. We installed the CCHP which was chosen as the most improved one. Only CCHP

could not meet the target, and recirculated air mix should be implemented for the cabin heating target. Although it could meet the heating performance target, it was worse than the baseline heat pump with high voltage PTC heater from the point of electric power consumption. It was caused by the higher pressure ratio and less COP. So we did some additional tests, in which the vapor injection, compressor rpm, and a low voltage auxiliary PTC heater were varying. And finally we could find out the optimum CCHP for cost effective CCHP system considering the cabin heating performance in cold climate, and electric power consumption. It was the CCHP with DPSC, vapor injection technique and low voltage PTC heater.

In conclusion, this study can help to guide the future CCHP development for EV application when you have to try to find proper techniques for CCHP considering package, cost and performance.

Appendix (*Kim H.S.*, 1998)

A. Modeling of scroll compressor volume

Geometric parameters used in the volume equations are shown in Table 2.

(1) Suction process $(0 < \text{ø} < 2\pi)$

$$V_{suc} = \frac{r \cdot \varepsilon \cdot h}{2} \cdot \left\{ \begin{array}{l} \phi \cdot (2\theta_e - \phi - \pi - \alpha_1 - \alpha_2) - 2(\theta_e - \pi - \alpha_1)\sin\phi \\ -\dfrac{(\pi - \alpha_2 + \alpha_1)\sin 2\phi}{2} + 2(1 - \cos\phi) \end{array} \right\} \qquad (1)$$

(2) Compression process

i) $2\pi < \text{ø} < \theta_e - \theta_A$

$$V_{comp} = \pi r \varepsilon h \cdot \left\{ 2(\theta_e - \phi) + \pi - \alpha_1 - \alpha_2 \right\} \qquad (\text{Eq.A 2}) \qquad (2)$$

ii) $\theta_e - \theta_A < \text{ø} < \text{ø}_e - 2\pi$

$$V_{comp} = h \cdot \left\{ A_1 - A_2 - A_3 - \frac{A_4}{2} - A_5 + \frac{A_6}{2} \right\} \qquad (3)$$

$$A_1 = \frac{r^2}{6} \cdot \left\{ (\theta_e - \phi + 2\pi - \alpha_2)^3 - (\theta_e - \phi + \pi - \alpha_2)^3 \right\} \quad (4)$$

$$A_2 = \frac{rt}{2} \cdot \left\{ (\theta_e - \phi + \pi)^2 - (\alpha_1 + \alpha_2)(\theta_e - \phi + \pi - \theta_A) - \theta_A{}^2 \right\} \quad (5)$$

$$A_3 = \frac{r^2\pi}{2} \cdot \left\{ (\theta_A - \alpha_1 - \frac{\pi}{2})^2 + \frac{\pi^2}{12} + 1 \right\} - \frac{(r_i^2 - r_o{}^2) \cdot (\pi - 2\beta)}{2} \quad (6)$$

$$A_4 = (r_i^2 - r_o{}^2) \cdot \left\{ \phi_e - \phi - 2\pi - \sin(\phi_e - \phi - 2\pi) \right\} \quad (7)$$

$$A_5 = \frac{r}{2} \cdot \left(2\varepsilon - \pi r + 2r\theta_0 - r\sin 2\theta_0 \right) \quad (8)$$

$$A_6 = r^2 \cdot \left(2\theta_0 - \sin 2\theta_0 \right) \quad (9)$$

$$\theta_0 = \cos^{-1}\left(\frac{\varepsilon}{2r} \right) \quad (10)$$

(3) Discharge process

i) $\phi_e - 2\pi < \phi < \theta_e - \theta_A + \pi$

$$V_{dis} = h \cdot \left\{ A_1 - A_2 - A_3 - A_4 - A_5 \right\} \quad (11)$$

$$A_1 = \frac{r^2}{6} \cdot \left\{ (\theta_e - \phi + 2\pi - \alpha_2)^3 - (\theta_e - \phi + \pi - \alpha_2)^3 \right\} \quad (12)$$

$$A_2 = \frac{rt}{2} \cdot \left\{ (\theta_e - \phi + \pi)^2 - (\alpha_1 + \alpha_2)(\theta_e - \phi + \pi - \theta_A) - \theta_A{}^2 \right\} \quad (13)$$

$$A_3 = \frac{r^2\pi}{2} \cdot \left\{ (\theta_A - \alpha_1 - \frac{\pi}{2})^2 + \frac{\pi^2}{12} + 1 \right\} - \frac{(r_i^2 - r_o{}^2) \cdot (\pi - 2\beta)}{2} \quad (14)$$

$$A_4 = (r_i^2 - r_o{}^2) \cdot \left\{ \phi_e - \phi - 2\pi - \sin(\phi_e - \phi - 2\pi) \right\} \quad (15)$$

$$A_5 = \frac{r}{2} \cdot \left(2\varepsilon - \pi r + 2r\theta_0 - r\sin 2\theta_0 \right) \quad (16)$$

$$A_6 = r^2 \cdot \left(2\theta_0 - \sin 2\theta_0 \right) \quad (17)$$

ii) $\theta_e-\theta_A+\pi < \phi < \theta_e-\theta_A+2\pi$

$$A_1 = \frac{r^2\pi}{2}\cdot\left\{(\theta_A-\alpha_1-\frac{\pi}{2})^2+\frac{\pi^2}{12}+1\right\}-\frac{(r_i^2-r_o^2)\cdot(\pi-2\beta)}{2} \tag{19}$$

$$A_2 = \frac{r^2}{6}\cdot\left\{(\theta_A-\alpha_1)^3-(\theta_e-\phi+\pi-\alpha_1)^3\right\} \tag{20}$$

$$A_3 = \frac{r^2}{6}\cdot\left\{(\theta_e-\phi+2\pi-\alpha_2)^3-(\theta_A-\alpha_2)^3\right\} \tag{21}$$

$$A_4 = \frac{r}{2}\cdot\left(2\varepsilon-\pi r+2r\theta_0-r\sin 2\theta_0\right) \tag{22}$$

$$A_5 = r^2\cdot\left(2\theta_0-\sin 2\theta_0\right) \tag{23}$$

iii) $\theta_e-\theta_A+2\pi < \phi < \phi_e$

$$V_{dis} = h\cdot(r_i^2-r_o^2)\left\{\phi_e-\phi-\sin(\phi_e-\phi)\right\} \tag{24}$$

References

Aikins K.A., Lee S.H., Choi J.M., 2013. Technology review Of two-stage vapor compression heat pump system. Int. Journal of Air-Conditioning And Refrigeration 21, 1330002

Bertsch S.S, Groll E.A., 2008, Two-stage air-source heat pump for residential heating and cooling applications in northern U.S.climates, , International journal of refrigeration, 31, 1282-1292.

Benouali J, heat pump architechtures for electric cars, SAE Thermal Management Systems Symposium, 2012

Chen Y., 2000, Mathematical modeling of scroll compressors, Ph.D.dissertation, University of Purdue.

Cho I.Y., Ko S.B., Kim Y.C., 2012, Optimization of injection holes in symmetric and asymmetric scroll compressors with vapor injection, International journal of refrigeration.

Choi Y.U., 2012. Studies on the performance characteristics of the vapor injection heat pump system in electric vehicle, M.S.dissertation, Seoul National University

Domanski P.A., 1995, Theoretical Evaluation of the Vapor Compression Cycle with a Liquid-Line/Suction-Line Heat Exchanger, Economizer, and Ejector, NIST, NISTIR 5606,Gaithersburg, MD, USA

He S., Guo W., Wu M. ,2006, Northern china heat pump application with the digital heatingscroll compressor, International Compressor

Engineering conference at Purdue, 116.

Hesse U., Results from CO_2 Heat pump applications, SAE Alternative refrigerant symposium, 2012

Heo J., Jung M., Kim Y., 2010, Improvement of the heating performance in a variable speed heat pump by applying the gas injection technique into a twin rotary compressor, International journal of refrigeration, 33, 848-855.

Heo J., Jung M.W.,Kim Y.C., 2010. Effects of flash tank vapor injection on the heating performance of an inverter-driven heat pump for cold regions. International Journal of Refrigeration 33, 848-855

Hirano T., Hagimeto K., Maeda M., 1990, Scroll Profiles for Scroll Fluid Machines, Mitsubishi Heavy Industries Technical Review, 27(1), 35-41.

Hosz M., Direk M., 2006. Performance evaluation of an integrated automotive air conditioning and heat pump system. Energy Conversion and Management 47, 545-559

Hunemorder W.,Nobuharu K., CO_2 heat pump system with electric compressor, VDA alternative refrigerant wintermeeting, 2003.

International Standard ISO917 : Testing of refrigerant compressors

Jang K.T., 2005, Study on the Thermodynamic Compression Process of Refrigerant in the Scroll Compressor with Heat Transfer Effect, Ph.D.dissertation, Korea Advanced Institute of Science and Technology.

John Rugh, Proposal for a vehicle level test procedure to measure air

conditioning fuel use, 2010-01-0799 SAE paper 2010

Kim H.S., 1998, A numerical study on the performance of the automotive scroll compressor using R-134a, Ph.D.dissertation, University of Sungkyunkwan.

Kwon C.K., Lee C.W., SAE 2014 Thermal management systems symposim , Thermal analysis of the vapor injection heat pump system for the future EV's possibilities

Kowsky C.,Wolfe E.,Leitzel L., Oddi F., Unitary HPAC system, SAE Int.J.Passeng. Cars, Cars-Mech.Syste.4(2):1016-025,doi:10.4271/2.12-01-1050

Lifson A., 2005, Novel vapor injection method for scroll compressors, London, UK. In: Proc. Int. Conference on Compressors and Their Systems, 381-390.

Liu Y., Hung C., Chang Y.C., 2009, Mathematical model of bypass behaviors used in scroll compressor, Applied Thermal Engineering, 29, 1058–1066

Ma G., Chai Q., 2004, Characteristics of an improved heat-pump cycle for cold regions, Applied Energy, 77, 235~247.

Ma G.Y., Zhao H.X., 2008, Experimental study of a heat pump system with flash tank coupled with scroll compressor, Energy and Buildings, 40, 697-701.

Mathison M.M., Braun J.E., Groll E.A., 2011, Performance limit for economized cycles with continuous refrigerant injection, International journal of refrigeration, 34, 234-242.

Myhre G., Shindell D., Bréon F.M., Collins W., Fuglestvedt J., Huang J., Koch D., J.-F. Lamarque, D. Lee, B. Mendoza, T. Nakajima, A. Robock, G. Stephens, T. Takemura and H. Zhang, 2013. Anthropogenic and Natural Radiative Forcing. In: Climate Change 2013: The Physical Science Basis. Contribution of Working Group I to the Fifth Assessment Report of the Intergovernmental Panel on Climate Change [Stocker, T.F., D. Qin, G.-K. Plattner, M. Tignor, S.K. Allen, J. Boschung, A. Nauels, Y. Xia, V. Bex and P.M. Midgley (eds.)]. Cambridge University Press, Cambridge, United Kingdom and New York, NY, USA.

Park C.H., Jee Y.J., Lee D.W., 2011, Development Trends of Heat-pump System for Electric Driven Vehicles, Auto Journal, 183, 29-35.

Park Y.C., Kim Y.C., Cho H.H., 2002, Thermodynamic analysis on the performance of a variable speed scroll compressor with refrigerant injection, International journal of refrigeration, 25, 1072-1082.

Roh C.W, Kim M.S, 2011, Effects of intermediate pressure on the heating performance of a heat pump system using R410A vapor-injection technique, International journal of refrigeration, 34, 1911-1921.

Roh C.W, Yoo J.W., Kim M.S. 2014. Vapor refrigerant injection techniques for heat pump systems : The latest literature review and discussion. Int. J. Air-Conditioning Refirgeration 22, 1430002

Roh C.W., Kim M.S., 2012. Macroscopic spray behavior and atomization characteristics of R407c injection. International Journal of Air-Conditioning Refrigeration 20, 1250009

SAE Standard J2765 : Procedure for Measuring System COP (Coefficient of Performance) of a Mobile Air Conditioning System on a Test Bench

Siddharth J., Gauray J., Clark B., 2004, Vapor injection in scroll compressors, International Compressor Engineering conference at Purdue, 2004.

Taras M.F., 2005, Is economizer cycle justified for AC applications, ASHRAE Journal, 47(7), 38-44.

Toshihisa K., Akira K., Hideki S., Masatoshi M., 2011, Development of Automotive Air-Conditioning Systems by Heat Pump Technology, Mitsubishi Heavy Industries Technical Review, 48(2), 27-32.

Tamura T., Yakumaru Y., Nishiwaki F., 2005. Experimental study on automotive cooling and heating air conditioning system using CO2 as a refrigerant. International Journal of Refrigerantion 28, 1302-1307

Umezu K., Suma S., 1984, Heat pump room air-conditioner using variable capacity compressor, ASHRAE Transactions, 90, 335-349.

Visteon heat pump system for hybrid and electric vehicle, 2012, http://www.greencarcongress.com/2012/09/visteon-20120929.html

Wang X., 2008, Performance Investigation of Two-stage Heat Pump System with Vapor Injected Scroll Compressor, Ph.D.dissertation, University of Maryland College Park.

Wang X., Hwang Y.H., Radermacher R., Pham H.M., 2008. Performance investigation of refrigerant vapor injection technique for residential heat pump system. Internaltional Refrigeration and Air Conditioning Conference at Purdue, West Lafayette IN.

Wawzyniak M., Benefits and challenges of heat pump system, SAE

Alternative refrigerant systems symposium, 2011

Winandy E.L., Lebrun J., 2002, Scroll compressors using gas and liquid injection: experimental analysis and modeling, International journal of refrigeration, 25, 1143-1156.

Xu X., Hwang Y.H, Reinhard R., 2011, Refrigerant injection for heat pumping/air conditioning systems: Literature review and challenges discussions, International journal of refrigeration, 34, 402-415.

Xing Xu, Hwang Y.H., 2011. Reinhard R., Refrigerant injection for heat pumping/air conditioning systems: Literature review and challenges discussions. International Journal of Air-Conditioning Refrigeration 34, 402-415

Yinhua Z., Brown M., Harry Y., Visteon Corp, A simple method to calculate vehicle heat load, 2011-01-0127 SAE paper 2011

Zhenquan L., Guirong, D., Zhiyoung, Q., 1992, The Graphic Method of Modified Wrap of Scroll Compressor, Proceedings of the International Compressor Engineering Conference at Purdue, 1099-1106.

초 록

배터리 구동 순수 전기차량은 주행거리 증대를 위해 고효율 난방시스템을 필요로 한다. 이때 공기열원 히트펌프는 냉방을 위해 사용하고 있는 에어컨 시스템을 공용으로 사용할 수 있고, 일반 전기히터보다 적은 에너지를 사용하기 때문에 효과적인 전기차 난방시스템이 될 수 있다. 하지만 외기온이 낮아지게 되면 히프펌프의 성능은 낮아질 수 밖에 없게 된다. 따라서 저온에서는 전기차에서 히트펌프를 적용하더라도 고전압 전기식 히터(PTC히터)와 같은 고용량 보조히터가 필요하다. 그러한 고용량 보조히터는 원가를 올릴 뿐 아니라, 엔진룸 내 패키지도 복잡하게 만든다. 따라서 전기차에 히트펌프 적용을 확대하고 원가 경쟁력 있는 전기차 개발을 위해서는 저온에서 히트펌프 성능 향상이 매우 중요하다. 이러한 저온 히트펌프(Cold climate heat pump, CCHP) 성능개선 연구는 건축이나 산업에서는 진행되어 왔으나, 전기차량용으로 연구는 제한적이다. 그래서 본 연구에서는 미래의 순수 전기차 적용을 위한 저온 히트펌프 방향을 연구하였고, 대표적인 저온 히트펌프 성능개선 기술인 기상냉매 주입(Vapor injection) 기술에 대해 차량용 시스템을 제안하고 스크롤 형상기반 열역학적 모델기반으로 해석적 연구를 수행하였다. 또한 3가지 형태의 저온 히트펌프 성능개선 방안을 제안하여 저온에서 성능개선을 실험적으로 확인하였다. 이때 먼저 시스템 레벨에서 실험이 진행되었고, 비정상상태 성능, 즉, 차량이 저온으로 담지(Soak) 후 웜업 과정에서 차량 열부하 변화를 고려한 차량단위의 평가도 진행하였

다. 이때 시스템 레벨 실험에서 선정된 최적안을 가지고 실차를 구성하였으며, 저온에서 웜업 상태의 난방성능과 그때 히트펌프 소모 동력을 비교 분석하였다. 결론적으로 이 연구를 통해 고비용 고용량 보조 히터(고전압 전기식 히터)를 대체할 저온 히트펌프(CCHP)의 가능성을 확인하였다.

주요어: 난방성능, COP, 히트펌프, 전기 자동차, vapor injection, cold climate, CCHP

학 번: 2010-30790